







Article

# Impacts of Warming and Acidification on Coral Calcification Linked to Photosymbiont Loss and Deregulation of Calcifying Fluid pH

Louise P. Cameron <sup>1,2</sup>, Claire E. Reymond <sup>2,3</sup> , Jelle Bijma <sup>4</sup> , Janina V. Büscher <sup>5</sup> , Dirk De Beer <sup>6</sup> , Maxence Guillermic <sup>7</sup> , Robert A. Eagle <sup>7</sup> , John Gunnell <sup>1</sup>, Fiona Müller-Lundin <sup>1</sup>, Gertraud M. Schmidt-Grieb <sup>5</sup>, Isaac Westfield <sup>1</sup>, Hildegard Westphal <sup>2,8,9</sup> and Justin B. Ries <sup>1,2,\*</sup>

<sup>1</sup> Department of Marine and Environmental Sciences, Northeastern University, Nahant, MA 01908, USA

<sup>2</sup> Leibniz Centre for Tropical Marine Research (ZMT), 28359 Bremen, Germany

<sup>3</sup> Geocoastal Research Group, School of Geosciences, The University of Sydney, Camperdown, Sydney, NSW 2006, Australia

<sup>4</sup> Alfred Wegener Institute, Helmholtz Center for Polar and Marine Research, Am Handelshafen 12, 27570 Bremerhaven, Germany

<sup>5</sup> GEOMAR Helmholtz Centre for Ocean Research Kiel, 24148 Kiel, Germany

<sup>6</sup> Max Planck Institute for Marine Microbiology, 28359 Bremen, Germany

<sup>7</sup> Atmospheric and Oceanic Sciences Department, Institute of the Environment and Sustainability, Earth, Planetary and Space Sciences, University of California, Los Angeles, CA 90095, USA

<sup>8</sup> Department for Geosciences, University of Bremen, 28359 Bremen, Germany

<sup>9</sup> Physical Science and Engineering Division, King Abdullah University of Science and Technology (KAUST), Thuwal, Makkah 23955-6900, Saudi Arabia

\* Correspondence: j.ries@northeastern.edu



**Citation:** Cameron, L.P.; Reymond, C.E.; Bijma, J.; Büscher, J.V.; De Beer, D.; Guillermic, M.; Eagle, R.A.; Gunnell, J.; Müller-Lundin, F.; Schmidt-Grieb, G.M.; et al. Impacts of Warming and Acidification on Coral Calcification Linked to Photosymbiont Loss and Deregulation of Calcifying Fluid pH. *J. Mar. Sci. Eng.* **2022**, *10*, 1106. <https://doi.org/10.3390/jmse10081106>

Academic Editor: Weidong Zhai

Received: 20 July 2022

Accepted: 6 August 2022

Published: 12 August 2022

**Publisher's Note:** MDPI stays neutral with regard to jurisdictional claims in published maps and institutional affiliations.



**Copyright:** © 2022 by the authors. Licensee MDPI, Basel, Switzerland. This article is an open access article distributed under the terms and conditions of the Creative Commons Attribution (CC BY) license (<https://creativecommons.org/licenses/by/4.0/>).

**Abstract:** Corals are globally important calcifiers that exhibit complex responses to anthropogenic warming and acidification. Although coral calcification is supported by high seawater pH, photosynthesis by the algal symbionts of zooxanthellate corals can be promoted by elevated pCO<sub>2</sub>. To investigate the mechanisms underlying corals' complex responses to global change, three species of tropical zooxanthellate corals (*Stylophora pistillata*, *Pocillopora damicornis*, and *Seriatopora hystrix*) and one species of asymbiotic cold-water coral (*Desmophyllum pertusum*, syn. *Lophelia pertusa*) were cultured under a range of ocean acidification and warming scenarios. Under control temperatures, all tropical species exhibited increased calcification rates in response to increasing pCO<sub>2</sub>. However, the tropical species' response to increasing pCO<sub>2</sub> flattened when they lost symbionts (i.e., bleached) under the high-temperature treatments—suggesting that the loss of symbionts neutralized the benefit of increased pCO<sub>2</sub> on calcification rate. Notably, the cold-water species that lacks symbionts exhibited a negative calcification response to increasing pCO<sub>2</sub>, although this negative response was partially ameliorated under elevated temperature. All four species elevated their calcifying fluid pH relative to seawater pH under all pCO<sub>2</sub> treatments, and the magnitude of this offset ( $\Delta[H^+]$ ) increased with increasing pCO<sub>2</sub>. Furthermore, calcifying fluid pH decreased along with symbiont abundance under thermal stress for the one species in which calcifying fluid pH was measured under both temperature treatments. This observation suggests a mechanistic link between photosymbiont loss ('bleaching') and impairment of zooxanthellate corals' ability to elevate calcifying fluid pH in support of calcification under heat stress. This study supports the assertion that thermally induced loss of photosymbionts impairs tropical zooxanthellate corals' ability to cope with CO<sub>2</sub>-induced ocean acidification.

**Keywords:** microelectrode; ocean acidification; global warming; calcifying fluid; scleractinian coral; zooxanthellate photosymbiont; photosynthesis; calcification; bleaching

## 1. Introduction

Anthropogenic emissions are predicted to cause sea-surface warming [1] and ocean acidification (OA)—a process that lowers seawater pH and aragonite saturation state [2] ( $\Omega_A$ ). OA increases both the dissolution rate of  $\text{CaCO}_3$  shell/skeleton [3] and the rate at which new shell/skeleton is formed [4]. Tropical scleractinian corals are carbonate producers [5] that acquire nourishment via symbiotic photosynthetic zooxanthellae and from heterotrophic feeding [6]. They are vulnerable to warming as many exist near the upper end of their thermal tolerance limits [7]. Warming beyond a coral's thermal tolerance may cause the loss of photosymbionts—a process known as bleaching.

Coral calcification occurs in the coral's calcifying fluid, which is influenced by both external seawater chemistry and the coral itself [8]. Corals elevate saturation state of this fluid through a combination of pH elevation via the active removal of protons using membrane-bound  $\text{Ca}^{2+}$ -ATPase proton pumps [8–14] and DIC elevation [15,16]. Photosynthesis may aid pH elevation by supplying the necessary ATP required to drive  $\text{Ca}^{2+}$ -ATPase proton pumps. Under ocean acidification, the formation of  $\text{CaCO}_3$  is more energetically costly [11,17,18], although this energetic cost is negligible compared to the total proportion of energy produced through photosynthesis [8]. Photosymbionts may therefore play a crucial role in mitigating the impacts of OA on corals by providing enough ATP to increase ion pumping rates in support of calcification. Photosynthesis may also be responsible for metabolic DIC elevation at the site of calcification, as implied by long-term seasonal variations in the concentration of DIC in the calcifying fluid [16]. Under warming, bleaching may impair coral calcification by reducing the amount of photosynthate that is translocated to the coral host, thereby increasing the coral's reliance on heterotrophic feeding [6], decreasing the metabolically derived DIC pool, and, potentially, reducing the amount of ATP available for proton-regulation in support of calcification.

Although tropical scleractinian corals generally exhibit parabolic calcification responses to ocean warming that are centered on their thermal optima [19], their calcification responses to OA are more nuanced. Many species exhibit reduced calcification rates [20,21], while others exhibit threshold responses [22], parabolic responses [19,21], or no calcification response to acidification [13,23,24].

This highlights the complexity of coral biomineralization, which can be biologically mediated by the secretion of skeletal organic molecules (SOM) such as adhesion, signaling, and structural proteins (e.g., calmodulin and sulphated acidic proteoglycans) [25–27]. The abundance of these SOMs in the calcifying fluid has been shown to alter the rate and morphology of aragonite precipitated [28–32].

Cold-water corals that inhabit deeper aphotic environments generally lack zooxanthellae and acquire nourishment exclusively through heterotrophic feeding [33]. The systems for regulating calcifying fluid pH ( $\text{pH}_{\text{CF}}$ ) within azooxanthellate corals may therefore differ from zooxanthellate corals. Azooxanthellate corals exhibit reduced skeletal density [34], reduced calcification rate [35], and altered rates of respiration and feeding [36] in response to OA, but increased calcification rates under elevated temperature [35,37].

Numerous studies have investigated the isolated effects of ocean acidification (e.g., [11,24,38,39]) and thermal stress (e.g., [40]) on coral  $\text{pH}_{\text{CF}}$ . However, the present study—along with its companion paper [41]—are the first to investigate both the independent and combined effects of warming and acidification on coral  $\text{pH}_{\text{CF}}$ . These empirical constraints, combined with photosymbiont and calcification data for the three tropical coral species, yield insight into the mechanism by which warming and acidification interact to so negatively impact coral growth. Examining the roles that  $\text{pH}_{\text{CF}}$  regulation and symbiont abundance play in the coral calcification response to OA and warming should improve understanding and prediction of how different species of corals will respond to future global change.

We investigate these relationships by culturing three species of tropical zooxanthellate corals (*Stylophora pistillata*, *Pocillopora damicornis*, *Seriatopora hystrix*) and one azooxanthellate cold-water species (*Desmophyllum pertusum*, syn. *Lophelia pertusa*) under control

(tropical = 28 °C, cold-water = 9 °C) and elevated (tropical = 31 °C, cold-water = 12 °C) temperatures at near-present-day (451–499 ppm), year 2100 (885–1096 ppm), and year 2500 (2807–3194 ppm) pCO<sub>2</sub> scenarios [1]. Coral calcifying fluid pH was measured with proton-sensitive microelectrodes. Symbiont abundance of the zooxanthellate corals was estimated based on coral color to investigate the role of photosymbionts in the coral calcification response to warming and acidification.

This work is a companion paper to Guillermic et al. [41], which investigated the impacts of pCO<sub>2</sub> and temperature on the calcifying fluid chemistry and calcification rate of two tropical species of scleractinian corals, *S. pistillata* and *P. damicornis*. The present study builds upon its companion paper by investigating these relationships for two additional species of scleractinian corals—the tropical species *S. hystrix* and the cold-water species *L. pertusa*. The present study also includes photosymbiont data for all three tropical coral species cultured under all experimental treatments.

## 2. Materials and Methods

### 2.1. Overview of Experimental Design

Three species of tropical scleractinian corals (*S. pistillata*, *P. damicornis*, and *S. hystrix*) were cultured under three ocean acidification (OA) scenarios established by modification of pCO<sub>2</sub> at control and elevated temperatures (control acidification: 28.29 °C ± 0.01 s.e./466 ppm ± 8; 31.72 °C ± 0.06/499 ppm ± 9; moderate acidification: 27.88 °C ± 0.02/925 ppm ± 15; 30.83 °C ± 0.02/885 ppm ± 12; high acidification: 28.17 °C ± 0.02/2807 ppm ± 119; 30.93 °C ± 0.02/3194 ppm ± 135) in four replicate tanks at each treatment for 62 days in April–June 2016 (Table 1). The control temperature treatment was assigned to fall within the natural temperature range of coral reefs in Fiji (26–29 °C), where these corals were collected [42]. Likewise, the elevated temperature was assigned to be just above the bleaching threshold (30–30.5 °C) for corals in Fiji [42]. Simultaneously, the cold-water coral *L. pertusa* was cultured under three OA scenarios at control and elevated temperatures (control acidification: 8.86 °C ± 0.02/451 ppm ± 24; 12.17 °C ± 0.03/494 ppm ± 16; moderate acidification: 9.07 °C ± 0.03/1096 ppm ± 99; 12.52 °C ± 0.04/1079 ppm ± 60; high acidification: 8.83 °C ± 0.02/2864 ppm ± 222; 12.67 °C ± 0.03/3167 ppm ± 202) in four replicate tanks at each treatment for 33 days in April–May 2016 (Table 2). Corals were acclimated to laboratory conditions for one week and then to experimental conditions for an additional two weeks prior to the start of the experiment. Calcification rates, pH<sub>CF</sub>, and relative photosymbiont abundance were quantified during the experiment (details below).

### 2.2. Coral Husbandry

Experiments were carried out in the MAREE marine experimental facility at the Leibniz Centre for Tropical Marine Research (ZMT). Specimens of the tropical scleractinian coral species *S. pistillata* and *P. damicornis* were obtained from DeJong MarineLife (Netherlands). Colony-level information was not available for these specimens. Specimens of the tropical scleractinian coral species *S. hystrix* were obtained from an experimental stock colony provided by the ZMT. Fragments of the cold-water coral *L. pertusa* were obtained from four colonies of an experimental stock culture provided by the Marine Biogeochemistry Department of the Helmholtz Centre for Ocean Research in Kiel (GEOMAR), previously collected at a depth of ca. 200 m at Nord-Leksa Reef in Trondheimsfjord, Norway. Coral fragments (*S. pistillata* = 65, *P. damicornis* = 63, *S. hystrix* = 52, and *L. pertusa* = 43) were mounted onto 3 cm × 3 cm plastic egg-crate stands using cyanoacrylate epoxy and assigned a unique identifier. Each treatment was replicated in four tanks. Equivalent size ranges of specimens were maintained across treatments. Coral specimens obtained from larger colonies were randomly distributed amongst pCO<sub>2</sub> and temperature treatments and replicate tanks. Coral specimens that died before the completion of the experiment were promptly removed from the tanks so as not to impact the remaining live corals in the experiment. Additional details about the number and weight of individuals in each treatment are provided in Section S1 of the Supplementary Online Material.

**Table 1.** Average calculated parameters for the tropical corals and all treatments: pCO<sub>2</sub> of the mixed gases in equilibrium with seawaters (pCO<sub>2</sub> (gas-e)), pH on seawater scale (pH<sub>SW</sub>), carbonate ion concentration ([CO<sub>3</sub><sup>2-</sup>]), bicarbonate ion concentration ([HCO<sub>3</sub><sup>-</sup>]), dissolved carbon dioxide ([CO<sub>2</sub>]<sub>SW</sub>), and aragonite saturation state (Ω<sub>A</sub>). Average measured parameters for all treatments: salinity (Sal), temperature (Temp), pH on NBS scale (pH<sub>NBS</sub>), total alkalinity (TA), and dissolved inorganic carbon (DIC). ‘SE’ represents standard error and ‘n’ is the sample size.

		400 ppm (9 °C)	400 ppm (12 °C)	1000 ppm (9 °C)	1000 ppm (12 °C)	2800 ppm (9 °C)	2800 ppm (12 °C)
<b>CALCULATED PARAMETERS</b>							
pCO <sub>2</sub> (gas-e)	(ppm-v)	466	499	925	885	2807	3194
	SE	8	9	15	12	119	135
	Range	362–540	425–607	808–1144	772–1050	1728–4302	2298–4945
	n	32	32	31	32	32	32
pH <sub>SW</sub>		8.11	8.06	7.85	7.87	7.42	7.42
	SE	0.02	0.02	0.01	0.01	0.01	0.02
	Range	8.03–8.30	7.97–8.27	7.73–7.98	7.80–7.99	7.28–7.51	7.20–7.57
	n	32	31	31	32	32	32
[CO <sub>3</sub> <sup>2-</sup> ]	(μM)	334	320	217	265	90	113
	SE	9	11	6	4	3	4
	Range	235–395	211–442	159–274	226–309	64–113	76–149
	n	32	32	31	32	32	32
[HCO <sub>3</sub> <sup>-</sup> ]	(μM)	2133	2017	2424	2468	2697	3030
	SE	33	36	35	35	77	54
	Range	1846–2433	1772–2389	2138–2748	2193–2842	2104–3289	2476–3475
	n	32	31	31	32	32	32
[CO <sub>2</sub> ] (sw)	(μM)	12.3	12.3	24.6	22.0	74.3	79.5
	SE	0.2	0.3	0.4	0.4	3.2	3.4
	Range	9–14	10–17	21–30	19–27	45–112	56–121
	n	32	32	31	32	32	32
Ω <sub>A</sub>		5.4	5.2	3.5	4.3	1.4	1.8
	SE	0.1	0.2	0.1	0.1	0.0	0.1
	Range	3.8–6.4	3.5–7.2	2.6–4.4	3.7–5.0	1.0–1.8	1.2–2.4
	n	32	32	31	32	32	32
<b>MEASURED PARAMETERS</b>							
Sal	(psu)	34.87	35.63	35.44	35.99	35.75	35.68
	SE	0.06	0.08	0.05	0.06	0.05	0.06
	Range	33.75–36.25	34.45–37.55	34.55–36.65	34.85–37.25	34.55–36.75	34.35–37.05
	n	104	104	104	104	104	104
Temp	(°C)	28.29	31.72	27.88	30.83	28.17	30.93
	SE	0.01	0.06	0.02	0.02	0.02	0.02
	Range	28.1–28.5	30.8–32.3	27.6–28.2	30.5–31.0	28.0–28.4	30.6–31.2
	n	104	104	104	104	104	104
pH <sub>NBS</sub>		8.27	8.24	8.04	8.12	7.62	7.69
	SE	0.01	0.01	0.01	0.01	0.01	0.01
	Range	8.02–8.47	8.12–8.48	7.88–8.33	7.92–8.34	7.47–7.98	7.48–7.97
	n	104	104	104	104	104	104
TA	(μM)	2915	2774	2939	3083	2907	3290
	SE	49	54	46	40	81	56
	Range	2420–3304	2309–3223	2524–3306	2735–3462	2260–3493	2705–3794
	n	32	32	32	32	32	32
DIC	(μM)	2480	2350	2645	2755	2861	3223
	SE	40	44	44	37	82	57
	Range	2097–2824	2009–2726	2013–3003	2445–3134	2231–3490	2634–3700
	n	32	32	32	32	32	32

**Table 2.** Average calculated parameters for *Lophelia pertusa* and all treatments: pCO<sub>2</sub> of the mixed gases in equilibrium with seawaters (pCO<sub>2</sub> (gas-e)), pH on seawater scale (pH<sub>SW</sub>), carbonate ion concentration ([CO<sub>3</sub><sup>2-</sup>]), bicarbonate ion concentration ([HCO<sub>3</sub><sup>-</sup>]), dissolved carbon dioxide ([CO<sub>2</sub>]<sub>SW</sub>), and aragonite saturation state (Ω<sub>A</sub>). Average measured parameters for all treatments: salinity (Sal), temperature (Temp), pH on NBS scale (pH<sub>NBS</sub>), total alkalinity (TA), and dissolved inorganic carbon (DIC). ‘SE’ represents standard error and ‘n’ is the sample size.

		400 ppm (9 °C)	400 ppm (12 °C)	1000 ppm (9 °C)	1000 ppm (12 °C)	2800 ppm (9 °C)	2800 ppm (12 °C)
<b>CALCULATED PARAMETERS</b>							
pCO <sub>2</sub> (gas-e)	(ppm-v)	451	494	1096	1079	2864	3167
	SE	24	16	99	60	222	202
	Range	238–580	399–595	672–1815	834–1496	1600–4162	1821–4669
	n	16	16	16	16	16	16
pH <sub>SW</sub>		8.20	8.21	7.87	7.86	7.42	7.42
	SE	0.04	0.04	0.04	0.03	0.04	0.03
	Range	8.01–8.54	7.96–8.40	7.62–8.12	7.70–8.06	7.17–7.67	7.19–7.63
	n	20	20	20	20	20	20
[CO <sub>3</sub> <sup>2-</sup> ]	(μM)	244	289	121	140	52	60
	SE	23	25	9	8	6	5
	Range	128–486	149–458	87–201	102–211	25–99	35–110
	n	20	20	20	20	20	20
[HCO <sub>3</sub> <sup>-</sup> ]	(μM)	2674	2775	2794	2835	3034	3058
	SE	107	111	89	95	69	81
	Range	2028–3356	2215–3348	2299–3366	2350–3349	2655–3420	2604–3486
	n	20	20	20	20	20	20
[CO <sub>2</sub> ] (sw)	(μM)	20	19	45	41	127	118
	SE	1	1	4	2	8	8
	Range	11–26	14–24	28–83	30–59	72–190	72–187
	n	20	20	20	20	20	20
Ω <sub>A</sub>		3.7	4.4	1.8	2.1	0.8	0.9
	SE	0.3	0.4	0.1	0.1	0.1	0.1
	Range	1.9–7.3	2.3–6.9	1.3–3.0	1.6–3.2	0.4–1.5	0.5–1.7
	n	20	20	20	20	20	20
<b>MEASURED PARAMETERS</b>							
Sal	(psu)	34.98	35.13	34.96	35.23	35.01	35.40
	SE	0.02	0.03	0.03	0.06	0.02	0.05
	Range	34.55–35.25	34.65–35.65	34.55–35.65	34.20–36.15	34.45–35.25	34.35–36.05
	n	60	60	60	60	60	60
Temp	(°C)	8.86	12.17	9.07	12.52	8.83	12.67
	SE	0.03	0.04	0.03	0.04	0.02	0.03
	Range	8.5–9.4	11.6–12.6	8.7–9.4	12.0–12.9	8.5–9.1	12.0–13.1
	n	60	60	60	60	60	60
pH <sub>NBS</sub>		8.07	8.13	7.80	7.82	7.39	7.40
	SE	0.01	0.02	0.02	0.02	0.02	0.02
	Range	7.82–8.39	7.85–8.43	7.48–8.15	7.52–8.01	7.13–7.75	7.12–7.63
	n	60	60	60	60	60	60
TA	(μM)	3245	3442	3080	3163	3157	3198
	SE	148	161	93	106	80	87
	Range	2355–4106	2601–4349	2598–3570	2609–3783	2752–3570	2759–3655
	n	20	20	20	20	20	20
DIC	(μM)	2938	3083	2960	3016	3214	3235
	SE	125	134	93	101	69	85
	Range	2180–3659	2395–3793	2449–3536	2494–3556	2805–3599	2741–3676
	n	20	20	20	20	20	20

After 1-week of acclimation at control conditions, temperature and pCO<sub>2</sub> were then incrementally increased to treatment levels over an additional week, after which time coral specimens were acclimated to treatment conditions for an additional week prior to the experiment. All coral specimens were cultured in 10-L replicate tanks supplied with seawater from 244-L sumps, where water filtration, temperature control, and pCO<sub>2</sub> control occurred. Seawater was filtered with protein skimmers, mechanical filters, and activated charcoal. All tropical coral aquaria were illuminated with 150 lux using actinic blue and white aquarium lights on a 12-h light/dark cycle. Aquaria holding the cold-water coral *L. pertusa* were not illuminated as this species lives below the photic zone. Each experimental treatment containing *L. pertusa* specimens (comprised of 4 replicate tanks) shared a water source with a separate reservoir containing five specimens of the king scallop *Pecten maximus* cultured as part of a separate experiment [43]. Seawater was filtered with protein skimmers, mechanical filters, and activated charcoal before returning to the *L. pertusa* tanks.

During acclimation and experimental periods, the tropical corals were fed 1-day old *Artemia salina* nauplii hatched from ca. 40 mg of eggs. Approximately 10 mL of concentrated live nauplii were introduced into each replicate tank every second day. The food mixture was pipetted directly adjacent to each coral specimen. Specimens of *L. pertusa* were fed the same diet supplemented with 20 mL of *Calanus finmarchicus* concentrate (Goldpods) suspended in the initial aliquot of *Artemia salina*. Corals were fed at the end of the day, and all filtration material was cleaned the following morning.

### 2.3. Seawater Chemistry Manipulation and Measurement

Measured and calculated carbonate system parameters are summarized in Tables 1 and 2. Experimental tank pCO<sub>2</sub> was maintained by vigorously bubbling mixtures of CO<sub>2</sub>-free air and CO<sub>2</sub> into the 244-L treatment sumps with microporous sparging tubes. The pCO<sub>2</sub> of the bubbled gases was achieved by mixing compressed CO<sub>2</sub>-free air and compressed CO<sub>2</sub> with solenoid-valve mass flow controllers at flow rates proportional to the target pCO<sub>2</sub> conditions. Natural seawater, originally collected from Spitsbergen, Norway, was continuously added to each of the 244-L sumps at a rate of 0.6 L/hour. Temperature (s.e.) for the tropical corals was maintained at 28 (0.02) °C and 31 (0.06) °C using 125-watt aquarium heaters (EHEIM), controlled with a programmable thermostat. Temperature for *L. pertusa* was maintained at 9 °C (0.03) and 12 °C (0.04) using aquarium chillers (Aqua Medic).

Temperature, pH, and salinity of all replicate tanks were measured three times per week using a multi-electrode probe (WTW Multi 3430 Set K). Samples for the analysis of dissolved inorganic carbon (DIC) and total alkalinity (TA) were collected weekly from each of the replicate tanks at midday and used to calculate other carbonate system parameters using the program CO2SYS [44]. Nutrient concentrations ([NO<sub>3</sub><sup>-</sup>], [PO<sub>4</sub><sup>3-</sup>], and [NH<sub>4</sub><sup>+</sup>]) of all replicate tanks were measured weekly. Additional details about the methods used to measure the carbonate system and nutrient concentrations of replicate tanks are provided in Section S2 of the Supplementary Online Materials.

### 2.4. Calcification Rates

Calcification rates were calculated from the change in estimated dry weight of all coral fragments over the experimental period. Dry weights were estimated from buoyant weight measurements taken at the start and end of the experimental period according to the following empirically derived relationships:

$$\textit{Stylophora pistillata}: \text{Dry weight (g)} = 1.919 \times \text{Buoyant Weight (g)} + 7.677;$$

$$\textit{Pocillopora damicornis}: \text{Dry weight (g)} = 1.662 \times \text{Buoyant Weight (g)} + 8.777;$$

$$\textit{Seriatopora hystrix}: \text{Dry weight (g)} = 1.668 \times \text{Buoyant Weight (g)} + 8.493;$$

$$\textit{Lophelia pertusa}: \text{Dry weight (g)} = 1.594 \times \text{Buoyant Weight (g)} - 0.206;$$



where the precision of this relationship is equivalent to the standard error of the regression (*S. pistillata*: 0.060 g; *P. damicornis*: 0.053 g; *S. hystrix*: 0.068 g; *L. pertusa*: 0.023 g). Additional details about the methods used to calculate calcification rate via buoyant weights are provided in Section S3 of the Supplementary Online Materials.

The number of days between the start and end buoyant weight measurements was then used to standardize %-calcification to a daily rate. Coral skeletons were also labeled with the fluorescent dye calcein (30 mg Se-Mark liquid calcein/kg-seawater) for 5 days prior to the initial buoyant weighing to identify skeletal material produced exclusively under the experimental conditions. Although all four species of corals recorded the calcein marker in their coral skeleton, rates of linear extension could not be reliably measured from the calcein marker because the dye was not incorporated into the skeletons in a consistent manner (see Section S4 of the Supplementary Online Materials for images of coral uptake of the calcein dye).

### 2.5. Estimating Coral Photosymbiont Index

The tropical coral specimens were photographed alongside the Coral Watch Coral Health Chart color scale [45–47] (Section S5 of the Supplementary Online Materials) under 150 lux (i.e., equivalent lighting to their experimental treatments) at the end of the experimental period to estimate relative photosymbiont abundance (a proxy for bleaching) of the coral specimens. This method involved extracting red-band color of the live coral tissue and the color scale and then assigning each pixel within the coral tissue image a discrete score (1–5) relative to the red-band values of the color scale (Figure 1). Additional details about the methods used to process photographs used for the estimation of photosymbiont index are provided in Section S5 of the Supplementary Online Materials.

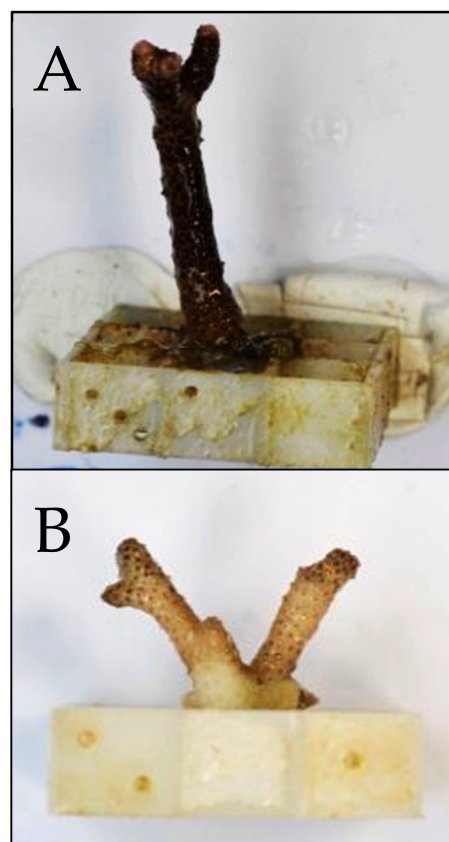


**Figure 1.** Representative images used in the estimation of relative photosymbiont abundance. Panel (A) depicts a healthy, unbleached coral from the control temperature, high pCO<sub>2</sub> treatment (color score = 5.69). Panel (B) depicts a partially bleached coral from the high temperature, high pCO<sub>2</sub> treatment (color score = 4.56).

### 2.6. Measurement of Calcifying Fluid pH

Calcifying fluid pH was measured using proton-sensitive liquid ion-exchanger (LIX) microelectrodes produced at the Max Planck Institute for Marine Microbiology (MPIMM) using a modified version of the technique described in De Beer et al. [48]. In brief, green soda lime glass microcapillary tubes (Schott model 8516) were held in a heated coil and pulled to a target tip diameter of ca. 10  $\mu\text{m}$ , yielding final diameters of 8–20  $\mu\text{m}$ . These were then silanized to produce a hydrophobic surface that allowed the adhesion of the LIX membrane. The microcapillary tubes were filled with ca. 300  $\mu\text{m}$  of degassed, filtered electrolyte (300 mM KCl, 50 mM sodium phosphate adjusted to pH 7.0) using a plastic syringe with a 0.1-mm tip. The microcapillary tubes were then backfilled with LIX containing a polyvinyl chloride (PVC) epoxy to prevent leakage of electrolyte by submerging the tips of the microcapillary tubes in LIX and apply suction to the other end of the tube until the PVC-containing LIX was drawn into the tip of the microcapillary by 100–200  $\mu\text{m}$ . Microcapillary tubes were encased in a Pasteur pipette for shielding, with the pulled tip of the microcapillary tube protruding ca. 2 cm beyond this casing. This casing was filled with a 0.3 M KCl solution and connected to the reference electrode with an Ag/AgCl wire to minimize electrical noise. Microelectrodes were left for 24 h after construction to allow for stabilization of the LIX membranes.

All microelectrode equipment (millivolt meter, National Instruments DAQ Pad 6020E, laptop, cables, micromanipulator, VT80 Micos motor arm, lab stands, Zeiss Stemi SV6 binocular microscope) was set up adjacent to the experimental tanks to minimize transport stress for the corals. Two reservoirs of seawater, sourced from the corresponding experimental treatment tanks, were established next to the microelectrode system. These reservoirs were bubbled with the corresponding treatment gases and maintained at the corresponding treatment temperature using aquarium heaters or chillers. The seawater was circulated between the two reservoirs through two 5.4 L flow-through chambers (30  $\times$  12  $\times$  15 cm). All pH microelectrode measurements were performed within these smaller flow-through chambers.

Measurements of calcifying fluid pH were made in the flow-through chambers filled with treatment seawater. Light levels in these chambers were measured using a digital lux-meter positioned next to the target coral polyp and were maintained at 150 lux. All corals were acclimated to the microelectrode chamber until polyp extension was observed prior to measurements (minimum of 10 min). Measurements of calcifying fluid pH were performed on three replicate individuals per treatment, with one measurement obtained for each individual. Calcifying fluid pH measurements were obtained for all species in all pCO<sub>2</sub> treatments under the control temperature treatment. Due to constraints on time and resources available for the experiment, calcifying fluid pH measurements under the high temperature treatment were only obtained for one species (*S. pistillata*).

The proton-sensitive LIX microelectrodes were used to measure both seawater and calcifying fluid pH. Before and after measurement of calcifying fluid pH, all microelectrodes were calibrated at the treatment temperature with pH 7 and 9 NBS buffers. The vertical position of the microelectrode was controlled with one-micron precision using a motorized micromanipulator. The microelectrodes were slowly inserted with a micromanipulator through the coral tissue into the upper portion of the coral calyx, between septal ridges and proximal to the thecal wall, until the skeleton was reached. This positioning of the electrode was verified by a shift in the pH profile [14] (Figure 2). A vertical pH profile (Figure 2) was then obtained by moving the microelectrode out of the calyx into the adjacent seawater. This profile was obtained in 1  $\mu\text{m}$  steps for the first 20  $\mu\text{m}$ , followed by 5  $\mu\text{m}$  steps out into the surrounding seawater.



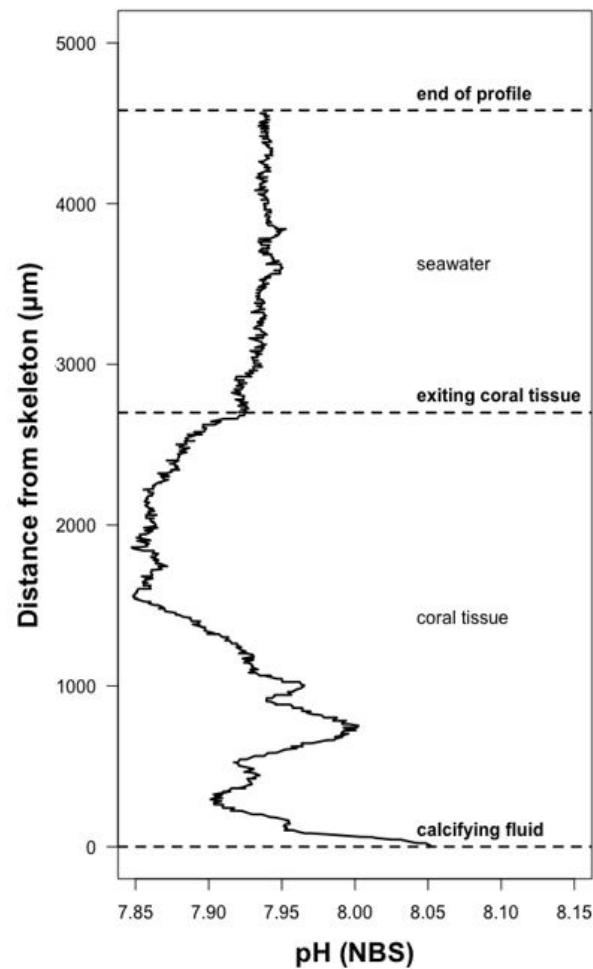


**Figure 2.** An example of a vertical pH profile generated during measurement of the coral calcifying fluid pH. This particular pH profile was generated for a specimen of *S. hystrix* cultured in the '1000 ppm pCO<sub>2</sub>, 28 °C' treatment.

The 1- $\mu\text{m}$  spatial resolution of the micromanipulator allowed for the positioning of the electrode within the thin calcifying fluid immediately adjacent to the coral skeleton. If the skeleton was inadvertently contacted during this positioning, it is possible that the tip of the microelectrode would break and render it dysfunctional. It was visually evident if the microelectrode tip broke upon contact with the skeleton, and this would also result in an abrupt voltage anomaly, often followed by a drift in the voltage even while the electrode was in a fixed position. The pH profile was aborted if there was evidence of any of these issues and then reinitiated with a new microelectrode.

The calibration and microelectrode pH data were processed by parsing scatter-plots of the data into three zones, which were annotated at the time of data collection. The calibration data were parsed as pH 7 buffer and pH 9 buffer. The microelectrode pH data were parsed as calcifying fluid, tissue, and seawater. Notes recorded during the original measurements were used to assist in identifying boundaries of adjacent zones. Measured mV within each zone of the calcifying fluid measurements were converted to pH using the calibration regression produced for each microelectrode. The  $\Delta[\text{H}^+]$  was calculated for each measured coral as the difference between the proton concentration ( $[\text{H}^+]$ ) of the coral's surrounding seawater and the  $[\text{H}^+]$  of the coral's calcifying fluid, both measured with the calibrated, proton-sensitive LIX microelectrodes.

## 2.7. Statistical Analysis

Statistical analyses were carried out in *R*. Corals that did not survive the experimental period (see Section S1 of the Supplementary Online Material) were excluded from analyses. A series of linear mixed effects models (lmers) were performed to investigate the influence of seawater pCO<sub>2</sub> and temperature on coral physiology (calcification rate, calcifying fluid pH, Δ[H<sup>+</sup>], photosymbiont index), with treatment tank specified as a blocking factor [49]. Akaike information criterion (AIC) was used to estimate the relative amount of information lost by any given model [50]. The final model was chosen based on the lowest AIC score (whereby a lower score reflects a better fitting model) and highest R<sup>2</sup>, which reflects the goodness of fit (from 0 to 1, 1 being a perfect fit) (see Section S6 of the Supplementary Online Material for AIC model selection tables). The normality and homoscedasticity of the chosen tests were then analyzed using diagnostic plots (QQ-plot, residuals vs. fitted plot), and normality was tested using a Shapiro–Wilk test. Color scores were square-root transformed to meet the assumption of normality. If an interaction term was significant, the individual levels of that interaction were examined in their own linear mixed effects models to interpret main effects.

Analysis of co-variance (ANCOVA) was used to investigate the impacts of seawater pCO<sub>2</sub>, temperature, and species on calcification rate, thereby allowing interspecific comparisons of the impacts of OA and warming on coral calcification rate. An ANCOVA was also used to make interspecific comparisons of the impact of OA on calcifying fluid pH and Δ[H<sup>+</sup>] of different coral species. The latter analyses excluded individuals from the elevated temperature treatment, as calcifying fluid pH was only obtained for one of the three coral species in this treatment.

Linear mixed effects models were used to examine the impact of photosymbiont index, as a proxy for photosymbiont abundance, on calcification rate. Multiple linear models were generated, starting with the model that contained the most terms (i.e., modeling calcification rate as a function of seawater pCO<sub>2</sub>, temperature, and photosymbiont index). Final interpretations of the data were based upon the models that maximized R<sup>2</sup> and minimized AIC (see Table S8). An alpha of 0.05 was used for all models, whereby any relationship with a *p*-value of <0.05 was deemed statistically significant.

## 3. Results

### 3.1. Predictors of Calcification Rate

The calcification rate of all coral species (Figure 3) was significantly impacted by the interaction between seawater pCO<sub>2</sub> and temperature (statistical significance indicated by *p*-value ≤ 0.05; Table S4). Calcification rate significantly increased with pCO<sub>2</sub> under control temperature for all three tropical species, but showed no change across pCO<sub>2</sub> treatments under elevated temperature for *S. pistillata* or *P. damicornis*, and decreased with increasing pCO<sub>2</sub> under elevated temperature for *S. hystrix*. Temperature had a significant negative effect on calcification rate in all tropical species (Table S4). Calcification rate of the cold-water azooxanthellate coral *L. pertusa* declined significantly with increasing pCO<sub>2</sub> at both temperatures, but showed a significantly stronger response to pCO<sub>2</sub> under the control temperature (Figure 3; Table S4).

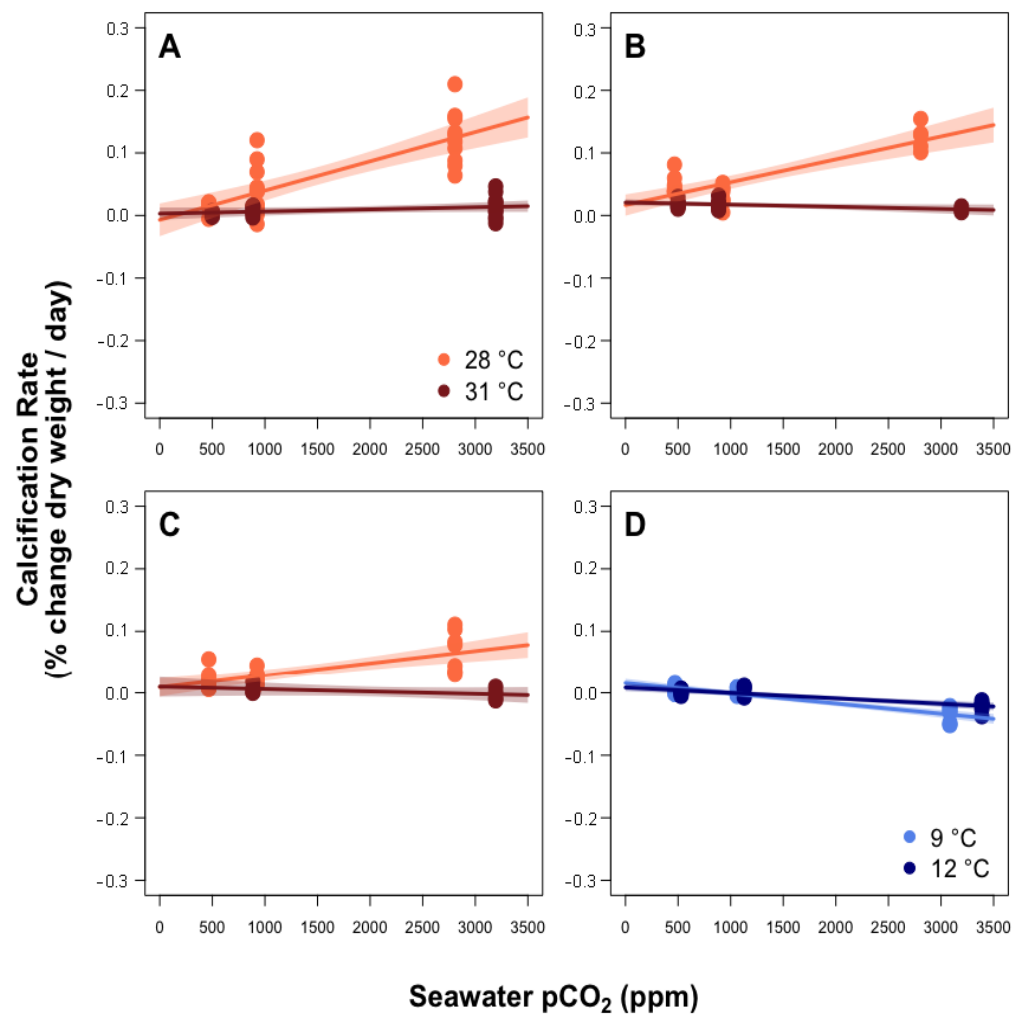


**Figure 3.** The relationship between  $p\text{CO}_2$  and coral calcification rates at ambient and high temperature ((A) = *S. pistillata*, (B) = *S. hystrix*, (C) = *P. damicornis*, and (D) = *L. pertusa*). Shaded boundaries represent 95% confidence intervals. Calcification rate was significantly impacted by an interaction between  $p\text{CO}_2$  and temperature for all coral species.

### 3.2. Calcifying Fluid Chemistry

The  $\text{pH}_{\text{CF}}$  of all four coral species was significantly greater than the  $\text{pH}$  of the corals' surrounding seawater ( $\text{pH}_{\text{SW}}$ ) after 30 days of exposure to ocean acidification and warming (Figure 4A–D; Imer, *S. pistillata*:  $p < 0.001$ ; *P. damicornis*:  $p = 0.002$ ; *S. hystrix*:  $p = 0.013$ ; *L. pertusa*:  $p = 0.002$ ). The  $\text{pH}_{\text{CF}}$  of all four species declined significantly with increasing  $p\text{CO}_2$  under control temperatures (Table S5), and, also, for *S. pistillata* under elevated temperature (*S. pistillata* was the only species for which  $\text{pH}_{\text{CF}}$  was measured at both control and elevated temperature; Figure 4). Under the elevated temperature treatment,  $\text{pH}_{\text{CF}}$  of *S. pistillata* remained higher than  $\text{pH}_{\text{SW}}$ , but was significantly lower than  $\text{pH}_{\text{CF}}$  at the control temperature (Table S5). The cold-water coral *Lophelia pertusa* exhibited the steepest decline in  $\text{pH}_{\text{CF}}$  with increasing  $p\text{CO}_2$  (Figure 5).

All four coral species increased their  $\Delta[\text{H}^+]$  (i.e., seawater  $[\text{H}^+]$ —calcifying fluid  $[\text{H}^+]$ ) in response to increasing seawater  $p\text{CO}_2$  (Figure 4E–H, Table S6). The  $\Delta[\text{H}^+]$  of *S. pistillata* was significantly influenced by the interaction between  $p\text{CO}_2$  and temperature (Table S6). In this species, there was no difference in  $\Delta[\text{H}^+]$  between the two temperature treatments under control  $p\text{CO}_2$ . The  $\Delta[\text{H}^+]$  increased with  $p\text{CO}_2$  under both temperature treatments, but this increase was significantly greater in the control temperature treatment.

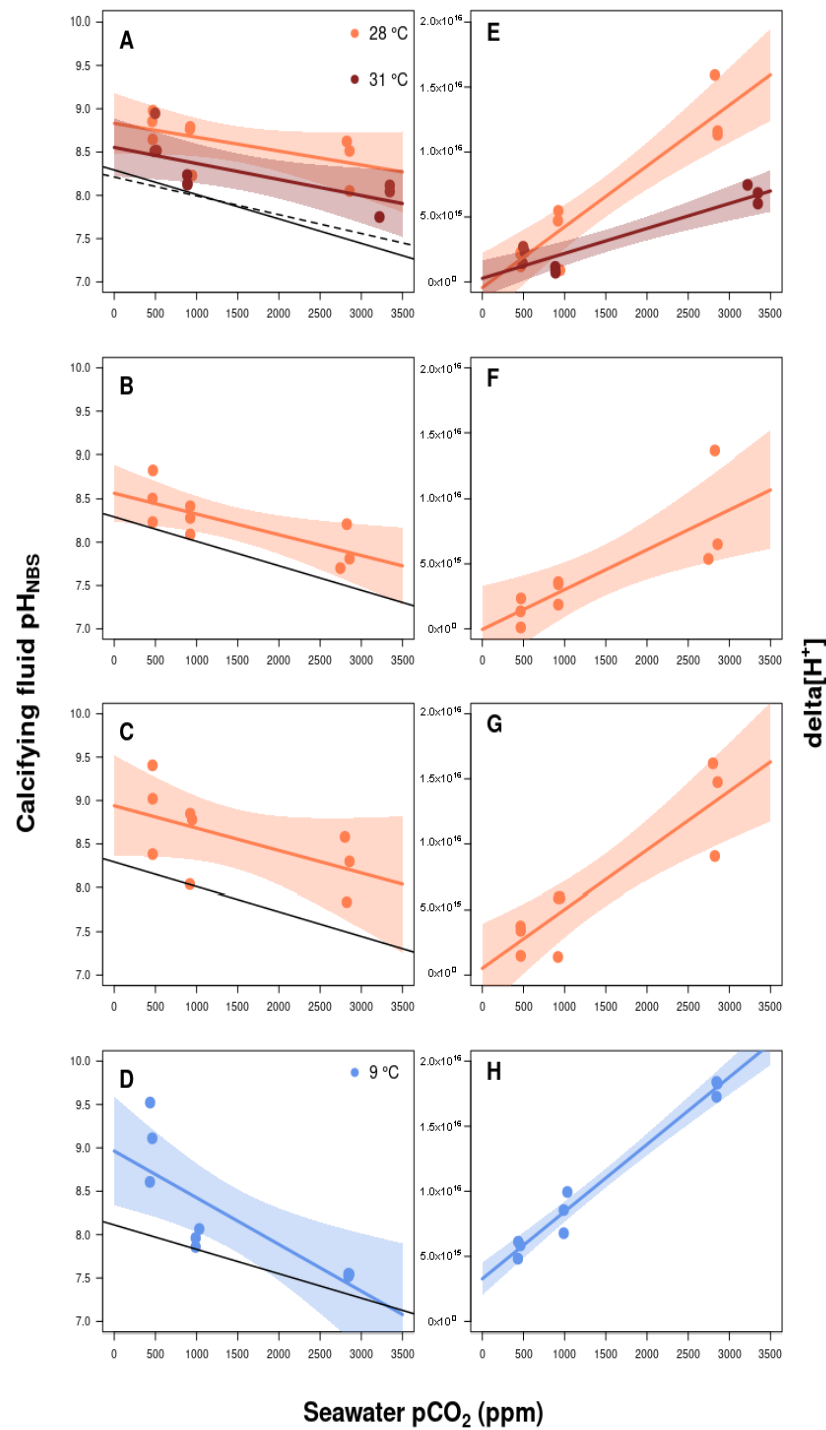


**Figure 4.** The effect of seawater pCO<sub>2</sub> on calcifying fluid pH (n = 3 individuals per treatment; panels (A–D)) and Δ[H<sup>+</sup>] (panels (E–H)) for three species of tropical corals ((A,E) = *S. pistillata*; (B,F) = *S. hystrix*, and (C,G) = *P. damicornis*) and one species of cold-water coral (*L. pertusa*; (D,H)). The impact of elevated temperature on the response of *S. pistillata* to increasing pCO<sub>2</sub> is also shown (panels (A) and (E)). Increasing pCO<sub>2</sub> was significantly associated with declining calcifying fluid pH and increasing Δ[H<sup>+</sup>] for all four coral species. The calcifying fluid pH of *S. pistillata* decreased significantly in response to a 3 °C increase in temperature, and Δ[H<sup>+</sup>] significantly responded to an interaction between increased pCO<sub>2</sub> and increased temperature. Shaded boundaries represent 95% confidence intervals. Solid black lines represent seawater pH under control temperature; dashed black line represents seawater pH under high temperature.

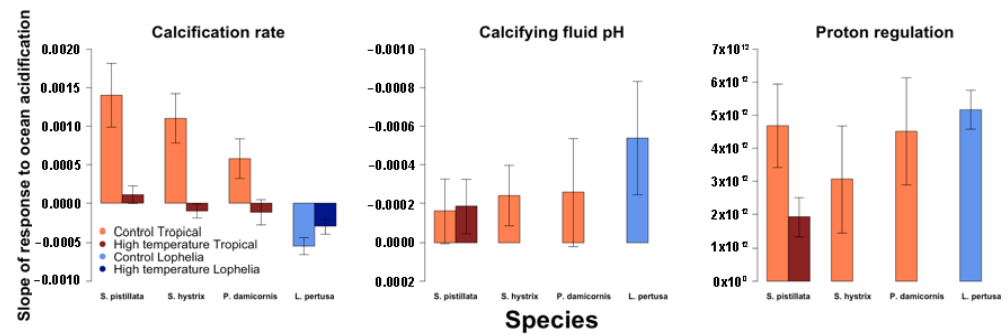


**Figure 5.** Slopes of regressions calculated from linear mixed effects models investigating the impacts of pCO<sub>2</sub> and temperature on calcification rate, calcifying fluid pH, and Δ[H<sup>+</sup>]. Significant differences were found amongst the slopes of the different coral species’ calcification responses to ocean acidification and warming. No significant difference was observed amongst the slopes of the different coral species’ calcifying fluid pH response to ocean acidification. The slopes of the different coral species’ proton regulation response (i.e., Δ[H<sup>+</sup>]) to ocean acidification were not significantly different from each other. Vertical bars represent 95% confidence intervals.

### 3.3. Estimated Coral Photosymbiont Index

Both *S. pistillata* and *P. damicornis* exhibited a lower photosymbiont index (i.e., lower estimated photosymbiont abundance) under the elevated temperature treatments (Figure 6, Table S7). Photosymbiont index significantly increased in both *S. pistillata* and *P. damicornis* when pCO<sub>2</sub> was elevated from control conditions (Figure 6, Table S7). The photosymbiont index of *S. hystrix* was significantly negatively correlated with the interaction between temperature and pCO<sub>2</sub>, whereby photosymbiont index increased significantly with increasing pCO<sub>2</sub> under the control temperature treatment, but showed no change in response to pCO<sub>2</sub> in the elevated temperature treatment.

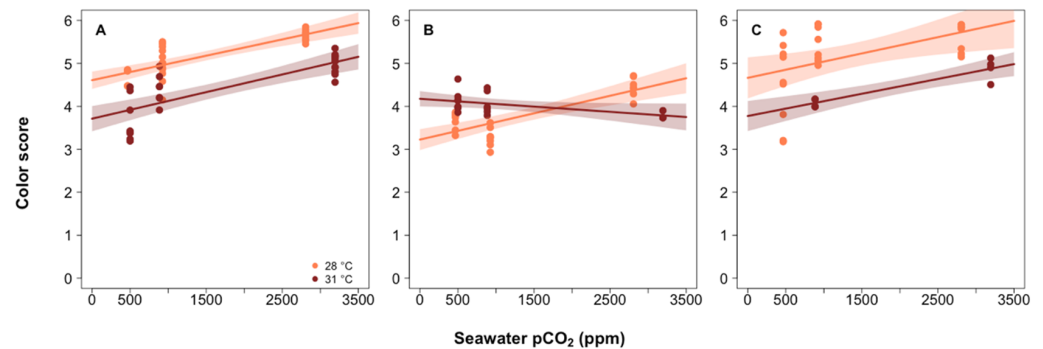


**Figure 6.** The effect of seawater pCO<sub>2</sub> and warming on the color score of the three species of tropical corals ((A): *S. pistillata*; (B): *S. hystrix*; (C): *P. damicornis*). Color score is a proxy for photosymbiont abundance (‘bleaching’), where 0 = bleached and 6 = healthy. Trendlines indicate significant correlations between seawater pCO<sub>2</sub> and color score at 28 (orange) and 31 (red) °C. The color score of both *S. pistillata* and *P. damicornis* increased in response to increasing pCO<sub>2</sub> (lmers, *S. pistillata*,  $p < 0.001$ ; *P. damicornis*,  $p = 0.001$ ) and decreased in response to a 3 °C temperature increase (lmers, *S. pistillata*,  $p < 0.001$ , *P. damicornis*,  $p = 0.001$ ). Color score of *S. hystrix* was significantly impacted (indicating bleaching) by an interaction between pCO<sub>2</sub> and temperature (lmer,  $p < 0.001$ ), whereby color score increased significantly with increasing pCO<sub>2</sub> at 28 °C (lmer,  $p < 0.001$ ) but showed no significant change with increasing pCO<sub>2</sub> at 31 °C (lmer,  $p = 0.056$ ). Shaded boundaries represent 95% confidence intervals.

### 3.4. Investigating the Role of Photosynthesis in Calcification

The calcification rate of *S. pistillata* was best predicted by the significant interaction between photosymbiont index and temperature, whereby photosymbiont index was pos-

itively correlated with calcification rate under both temperatures, but the slope of this correlation was significantly greater under the control temperature treatment (Figure 7A, Table S8). The calcification rate of *S. hystrix* was best predicted by a model that included both photosymbiont index and temperature independently. Photosymbiont index had a positive linear relationship with calcification rate under both temperatures, but the slope of this relationship significantly decreased in the high temperature treatment (Figure 7B, Table S8). The calcification rate of *P. damicornis* was best predicted by a model that contained photosymbiont index, seawater pCO<sub>2</sub>, and temperature (Table S8). The only significant predictor of calcification rate of *P. damicornis* was the interaction between photosymbiont index, temperature, and pCO<sub>2</sub> (Figure 7C, Table S8).

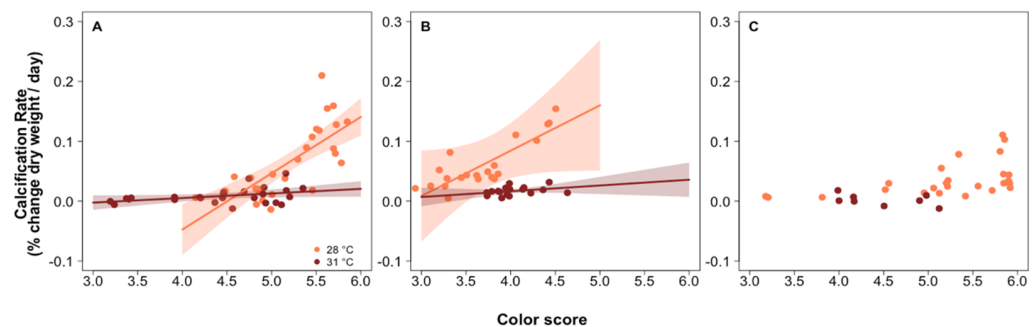


**Figure 7.** The relationship between coral color score and calcification rate of three species of tropical corals ((A): *S. pistillata*; (B): *S. hystrix*; (C): *P. damicornis*). Color score is a proxy for photosymbiont abundance ('bleaching'), where '0' = bleached and '6' = healthy. Trendlines indicate significant correlations between color score and calcification rate at 28 (orange) and 31 (red) °C. Temperature significantly impacted the relationship between color score and calcification rate of *S. pistillata*, and caused a significant decline in calcification rate of *S. hystrix*. No significant relationship existed between calcification rate and color score of *P. damicornis*, and temperature had no significant impact on this relationship. Shaded boundaries represent 95% confidence intervals.

## 4. Discussion

### 4.1. Calcification Response to pCO<sub>2</sub> and Thermal Stress

Prior studies have shown that *S. pistillata* and *P. damicornis* both exhibit resilience in their calcification response to ocean acidification [13,51,52], while *S. hystrix* [53] tends to exhibit more negative responses. The present study, however, shows that, in the absence of thermal stress, these three common species of tropical zooxanthellate corals exhibit increased rates of calcification in response to a one-month exposure to CO<sub>2</sub>-acidified conditions. Although the disparity between the results of the past and present studies on these species could be due to differences in experimental design, such as experimental duration, the method used to measure calcification rates, temperature treatments, and/or light levels, these findings provide compelling evidence that, under certain circumstances (e.g., absence of thermal stress), some tropical zooxanthellate coral species can tolerate OA over at least one-month intervals.

Under the elevated temperature treatment (31 °C), the calcification rates of all three tropical coral species were reduced compared to the control temperature, but were unchanged by increasing pCO<sub>2</sub>, showing that thermal stress effectively impaired the zooxanthellate corals' calcification response to CO<sub>2</sub>-induced OA. However, it should be noted that warming can have either positive or negative effects on coral calcification rate, depending on whether the warming causes temperatures to approach or exceed, respectively, the coral's thermal optimum [19,21,54,55].

Few studies have investigated the calcification response of corals to combined ocean acidification and warming. While some of the studies show a negative response to these combined stressors [55], others contrast the results of the present study by showing no interactive effects of ocean acidification and warming [21,56,57]. The results presented here



show that the impacts of ocean acidification on the calcification rates of three *Pocilloporid* coral species are exacerbated by warming. Because OA and global warming typically occur in tandem during major perturbations to the Earth's carbon cycle, both throughout Earth history [58] and as a consequence of anthropogenic CO<sub>2</sub> emissions [59], future CO<sub>2</sub>-induced global change poses a substantial threat to these coral species.

The calcification rate of the cold-water azooxanthellate coral *L. pertusa* declined under elevated pCO<sub>2</sub> at both temperatures. This negative calcification response to pCO<sub>2</sub> was weaker under the elevated temperature. Notably, the direction of the pCO<sub>2</sub>-temperature interaction for the cold-water azooxanthellate species was opposite that of the three tropical species. *Lophelia pertusa* exhibited net dissolution when seawater pCO<sub>2</sub> reached ca. 1000 ppm, although low levels of calcification have been previously observed for *L. pertusa* under similar conditions [34,35,60]. These conditions are predicted to occur in the surface open ocean by the end of the 21st century [1] and earlier in high-latitude cold-water environments [61]—suggesting that this cold-water ecosystem engineer, whose reef-systems function as nursery ground for a number of commercially important fish species [62], may be unable to form reefs beyond this century. However, the observation that increased temperature partially mitigates the impact of OA agrees with the results of longer-term studies [35], and suggests that the impacts of global change on this species will vary with temperature across latitude and depth, as this species can inhabit seawater ranging from 4 to 14 °C [63,64].

The differences in calcification response to ocean acidification shown here may arise from differences in the physiology and ecology of tropical vs. cold-water corals. Although tropical corals exist close to their thermal limits and are therefore vulnerable to even small amounts of warming, azooxanthellate cold-water corals can generally tolerate a wider temperature range [65]. Elevated respiration rates have been observed for *L. pertusa* in warmer temperatures [66]. Thus, an increase in temperature may boost metabolic rates to partially mitigate the impacts of OA on calcification in the high pCO<sub>2</sub> treatments. The species of tropical corals studied here are colonial and, thus, share resources between closely packed polyps [67]. These polyps are connected by coenosarc tissue, which covers and protects the skeleton [68]. The high degree of tissue cover exhibited by tropical corals means that the skeleton is well protected from dissolution, which may explain the lack of negative calcification response (i.e., lack of net dissolution) for the tropical corals in this study. Their shared gastrovascular system allows the distribution of metabolites generated from coral respiration and zooxanthellate photosynthesis across the colony, which could yield further resilience against ocean acidification. In contrast, *L. pertusa* is a pseudocolonial species [69] that produces single polyps on the end of stalk-like branches. The coenosarc connecting these branches is often partially absent in laboratory specimens and in wild specimens during the winter, leaving regions of exposed skeleton vulnerable to dissolution [65]. This lack of connectivity between polyps and the presence of exposed skeleton may increase the vulnerability of *L. pertusa* to ocean acidification.

Alternatively, the increased solubility of CO<sub>2</sub> in colder waters caused  $\Omega_A$  of the *L. pertusa* treatments to be 0.12–0.70 units lower at 9 °C than at 12 °C for a given pCO<sub>2</sub> condition. This may have caused higher rates of skeletal dissolution in the high-pCO<sub>2</sub> treatments maintained at the lower temperature, although the rate of dissolution of coral skeletons should be higher under the higher temperature treatments for equivalent  $\Omega_A$  [3]. Since the buoyant weight method [70] used here yields only a net rate of calcification, i.e., mass of new skeleton produced through gross calcification minus mass of exposed skeleton lost through gross dissolution, it is not possible to determine whether the positive impact of the interaction between pCO<sub>2</sub> and temperature on *L. pertusa* calcification rate was driven by increased gross calcification or reduced gross dissolution (or a combination of these factors) in the high-temperature, high-pCO<sub>2</sub> treatments. Additionally, it was not determined whether OA impacted the density of coral skeleton, which could increase the fragility of the reef framework that these corals form [71].

The responses observed in the present study are consistent with other laboratory studies showing that scleractinian corals exhibit a wide range of calcification responses to OA [13,19–24,52,72]. Some of this variability may arise from differences in experimental design, such as the amount of food provided to the corals, the levels of irradiance, and the duration of the experiment. Nevertheless, this high variability in calcification response patterns across and within species indicates that a greater understanding of the mechanisms that drive coral responses to OA is needed.

The present study was conducted over an eight-week interval, with a total of three weeks of acclimation to laboratory and experimental conditions, and should, therefore, be considered intermediate in duration. As with any experimental OA study, it is possible that the duration of exposure may influence results, as corals may function normally over short timeframes, but exhibit impaired function over longer timeframes as a result of cumulative stress and/or depletion of metabolic resources [19]. Alternatively, corals may exhibit impaired responses shortly after exposure to the treatment conditions due to shock, but acclimate to the treatment conditions over longer timeframes. Prior laboratory-based studies have shown that tropical corals exhibit variable degrees of acclimation to OA over relatively short timescales [19,24,73], whereas acclimation of *L. pertusa* has been observed over longer timescales [74]. The large inter- and intra-specific differences in coral response to OA across experiments and timeframes underscores the need for additional research into the long-term effects of OA on coral calcification.

#### 4.2. Role of Calcifying Fluid pH Regulation in Coral Response to $p\text{CO}_2$ and Thermal Stress

Coral calcifying fluid pH elevation has been widely cited as a mechanism for promoting calcification under conditions of ocean acidification [8,11,14]. Although  $\text{pH}_{\text{CF}}$  declined in all four species under elevated  $p\text{CO}_2$ , it always remained higher than  $\text{pH}_{\text{SW}}$ . Notably, coral species that showed the highest degree of control over  $\text{pH}_{\text{CF}}$  in the present experiment, and thus the shallowest slope of change in  $\text{pH}_{\text{CF}}$  in response to changing seawater  $p\text{CO}_2$ , also exhibited the greatest increase in calcification rate when  $p\text{CO}_2$  was increased, suggesting that  $\text{pH}_{\text{CF}}$  regulation confers resilience to corals exposed to OA.

These trends are consistent with prior estimation of coral  $\text{pH}_{\text{CF}}$  from boron isotopes [10,38,39,41,75–77], pH-sensitive fluorescent dyes [12], and pH-sensitive microsensors [9,11]. Previous studies of the effects of ocean acidification on calcification site pH show that both *S. pistillata* and *P. damicornis* elevate  $\text{pH}_{\text{CF}}$  above seawater pH, and that this elevation increases under ocean acidification [13,52]. These results are consistent with the findings here, although the measured  $\text{pH}_{\text{CF}}$  was considerably higher in the present study compared to previous studies.

The present study used pH-sensitive microelectrodes, whereas prior studies on both *S. pistillata* and *P. damicornis* [52], and *P. damicornis* [13] used confocal microscopy to image pH-sensitive SNARF-1 dye in coral microcolonies grown on glass slides and boron isotope systematics, respectively. Differences in  $\text{pH}_{\text{CF}}$  could be due to differences in methods of culturing and/or  $\text{pH}_{\text{CF}}$ -estimation, or due to genotypic differences between cultured specimens. Of the three methods used to estimate  $\text{pH}_{\text{CF}}$  (pH-sensitive dyes, boron isotopes, and pH-sensitive microelectrodes), pH-sensitive microelectrodes typically yield the highest  $\text{pH}_{\text{CF}}$  [11], although a side-by-side comparison of  $\text{pH}_{\text{CF}}$  measured with pH-sensitive dye and pH microelectrodes on the same specimens yielded comparable results [14].

Measurements of  $\text{pH}_{\text{CF}}$  using pH-sensitive microelectrodes are challenged by the difficulty in assessing the precise location of the microelectrode tip relative to the coral's calcifying fluid. This challenge was addressed in the present experiment through the creation of  $\text{pH}_{\text{CF}}$  profiles as the pH microelectrode was withdrawn from the calcifying fluid, thus allowing characterization of the calcifying fluid pH compared to intratissue and/or gastrovascular pH (Figure 2), as was conducted in previous studies [14,78]. Additionally, the  $\text{pH}_{\text{CF}}$  of two coral species in the present study (*S. pistillata* and *P. damicornis*) was estimated by coral skeletal  $\delta^{11}\text{B}$  to provide a side-by-side comparison of these independent approaches to measuring  $\text{pH}_{\text{CF}}$  [41]. A significant correlation was found between  $\text{pH}_{\text{CF}}$

measured using these two methods, increasing confidence that the measurements obtained here represent pH of the calcifying fluid. The offset between the two approaches was attributed to the two techniques measuring  $\text{pH}_{\text{CF}}$  over different timescales—with skeletal  $\delta^{11}\text{B}$  recording a time-averaged value of  $\text{pH}_{\text{CF}}$  and pH microelectrodes recording a more instantaneous value of  $\text{pH}_{\text{CF}}$  [41].

Although numerous studies have shown that OA reduces coral  $\text{pH}_{\text{CF}}$ , few have investigated the combined impact of warming and OA on  $\text{pH}_{\text{CF}}$ . In the present study, microelectrode measurements of the  $\text{pH}_{\text{CF}}$  of *S. pistillata* were measured in all  $\text{pCO}_2$  and temperature treatments. The prescribed temperature increase resulted in a significant decline in  $\text{pH}_{\text{CF}}$  for each of the three  $\text{pCO}_2$  treatments. Under heat stress, corals may receive less nourishment from their photosymbionts to support  $\text{pH}_{\text{CF}}$  regulation due to thermally induced bleaching and/or may divert energy from the regulation of  $\text{pH}_{\text{CF}}$  towards tissue repair.

Assuming that the coral calcifying fluid is ultimately derived from the coral's surrounding seawater [79], the extent to which a coral mitigates the impacts of OA by removing protons from its calcifying fluid can be grossly estimated (excluding the effects of buffering) from the difference between the  $[\text{H}^+]$  of the calcifying fluid and the  $[\text{H}^+]$  of the surrounding seawater (i.e.,  $\Delta[\text{H}^+]$ ). All four coral species exhibited increased  $\Delta[\text{H}^+]$  under elevated  $\text{pCO}_2$  treatments, suggesting that more energy is allocated to  $\text{pH}_{\text{CF}}$  regulation under elevated  $\text{pCO}_2$ . The  $\Delta[\text{H}^+]$  was lower in the high-temperature treatment in *S. pistillata*, suggesting that less energy is available to maintain elevated  $\text{pH}_{\text{CF}}$  when the corals experience thermally induced symbiont loss—potentially due to a commensurate decrease in photosynthate translocated to the coral host.

#### 4.3. Role of Photosymbionts in Coral Response to $\text{pCO}_2$ and Thermal Stress

In order for corals to allocate more energy toward removing protons from their calcifying fluid under OA conditions, they must divert energy from other activities and/or increase their energetic intake [80]. Zooxanthellate corals obtain energy from two sources—heterotrophic feeding and photosynthate translocated from their algal symbionts. As corals are sessile suspension feeders, they are limited in the extent to which they can increase heterotrophic feeding, although they may increase feeding rates if sufficient food is available [81,82]. Alternatively, enhanced photosynthesis under OA may play an important role in driving proton elevation under OA.

Using the well-established colorimetric method of Siebeck et al. [45] to estimate the abundance of zooxanthellae via the photosymbiont index, it was shown that the populations of photosymbionts from *S. pistillata* and *P. damicornis* were significantly reduced in the high temperature treatment compared to the initial values. This is consistent with prior work showing that prolonged heat stress can lead to expulsion of zooxanthellate and tissue damage, a process termed 'bleaching' [83]. However, in this study, the photosymbiont index increased in response to increasing  $\text{pCO}_2$  under both temperature treatments, suggesting that the photosymbionts within all three *Pocilloporid* tropical corals benefited from the increased availability of dissolved inorganic carbon (DIC). The alleviation of carbon limited photosynthesis could free up energy for elevating  $\text{pH}_{\text{CF}}$  and/or the production of carbon concentrating enzymes (e.g., carbonic anhydrase [84]), thereby aiding calcification under the control temperature [68,85,86]. The zooxanthellae's apparently positive response to increasing DIC also suggests that dissolved inorganic nutrients (DIN) were sufficient and in the correct balance (i.e., Redfield ratio) to sustain photosynthesis [87,88]. This link between enhanced photosynthesis and enhanced calcification under the elevated  $\text{pCO}_2$  and control temperature treatment is consistent with the observed correlations between photosymbiont index and calcification rate in *S. pistillata* and *S. hystrix* across all treatments.

#### 4.4. Proposed Mechanistic Framework for Zooxanthellate Coral Response to pCO<sub>2</sub> and Thermal Stress

We propose the following mechanistic framework to explain the zooxanthellate coral responses to OA and warming observed in this study. Under the control temperature and pCO<sub>2</sub> conditions, zooxanthellae fix DIC as carbohydrates (photosynthate), which is then used by the coral hosts as an energy source for all physiological activities, including elevation of pH<sub>CF</sub> in support of calcification [4,8,89,90]. When OA occurs without thermal stress, high pCO<sub>2</sub> enhances photosynthesis in the coral species investigated and increases their photosymbiont index. Under conditions of elevated pCO<sub>2</sub>, enhanced photosymbiont productivity (evidenced by increased photosymbiont index in this study), will result in a greater abundance of byproducts that may be used by the coral host to increase proton removal from the calcifying fluid (evidenced by elevated  $\Delta[\text{H}^+]$ ). The combination of elevated pH<sub>CF</sub> and elevated DIC (due to elevated pCO<sub>2</sub>) under OA conditions may allow some species of corals to maintain an  $\Omega_A$  in their calcifying fluid that is comparable to or, perhaps, greater than those exhibited under non-acidified conditions [11]—hence, their observed ability to maintain constant or, in some cases, elevated rates of calcification under OA.

Although CO<sub>2</sub>-induced OA appears supportive of calcification for these three species under the control temperature, this support breaks down in the high temperature treatment. The thermal stress induced in this treatment caused a reduction in the abundance of the corals' algal symbionts (evidenced by their reduced photosymbiont index), which was accompanied by a reduction in  $\Delta[\text{H}^+]$  (i.e., proton removal) and calcification rate of *S. pistillata* under each of the elevated pCO<sub>2</sub> treatments. It appears that the thermally induced reduction in photosymbiont index eliminated the benefit of enhanced photosynthesis under conditions of elevated pCO<sub>2</sub>, thereby leaving the coral with fewer resources (e.g., translocated photosynthate) for elevating pH<sub>CF</sub>. It should also be noted that thermal impairment of the enzymes used to remove protons from the coral calcifying fluid (e.g., H<sup>+</sup>/Ca<sup>2+</sup>-ATPase [9,91]) may have contributed—along with reduced photosymbiont index—to declines in pH<sub>CF</sub> and  $\Delta[\text{H}^+]$  observed for *S. pistillata* in response to thermal stress. Additionally, the different responses shown in the control and high temperature treatments could be due to a temperature-induced shift in the strategy used by the coral to elevate aragonite saturation state in their calcifying fluid. In natural reef systems, it has been shown that coral pH<sub>CF</sub> is most elevated in the winter months [16]. Although pH<sub>CF</sub> is still elevated in the warmer summer months, it is elevated to a lesser extent, and DIC elevation appears to be the primary means of raising  $\Omega_A$  [16]. These observations are consistent with and provide a potential explanation for the results of the present study.

The role of symbiotic zooxanthellae in conferring resilience to corals exposed to OA is also highlighted in the stark contrast observed between the tropical and deep-sea coral responses to OA. Cold-water corals are azooxanthellate and thus do not receive the benefits of enhanced symbiont photosynthesis under elevated pCO<sub>2</sub>. Although  $\Delta[\text{H}^+]$  of the cold-water species was comparable to that of the tropical species under OA, proton regulation of the calcifying fluid probably consumes a greater proportion of the total resources of the cold-water species (which acquires no resources from photosynthesis) than that of the tropical zooxanthellate species. This may leave proportionally fewer resources (compared with the tropical species) for other processes associated with calcification in the cold-water species, such as the production of organic matrices that may initiate crystal nucleation [92], which may explain the more negative calcification response to OA exhibited by *L. pertusa*.

#### 4.5. Limitations of Laboratory-Based Experiments

The results described here were obtained in a controlled laboratory setting. In their natural reef environments, tropical corals experience fluctuations in temperature and carbonate chemistry across daily [93–95] and seasonal [96,97] cycles, whereas corals inhabiting deeper, colder waters experience more stable environments. Thus, differing degrees of prior exposure to fluctuations in pH could contribute to the differential responses of the tropical

and cold-water coral species observed here. The enhanced decline in  $\text{pH}_{\text{CF}}$  under elevated temperature exhibited by the tropical corals could also result from a shift in strategy for elevating calcifying fluid  $\Omega_{\text{A}}$  from  $\text{pH}_{\text{CF}}$  elevation to DIC elevation, as has been shown to occur seasonally in a natural reef system [16]. Future research is necessary to assess whether the responses observed here hold in more dynamic temperature and pH environments.

## 5. Conclusions

Global warming is considered to be amongst the greatest threats facing coral reefs, and OA is emerging as an equally grave threat. We show that warming has a more negative impact than OA on three species of zooxanthellate tropical corals, whereas OA has a more negative impact than warming on an azooxanthellate cold-water coral. This study also provides insight into the role of photosymbionts in corals' response to OA. Specifically, the enhancement of symbiont photosynthesis under higher- $\text{pCO}_2$  conditions appears to mitigate the negative effects of OA on tropical zooxanthellate corals by providing resources that assist in the maintenance of elevated calcifying fluid pH in support of calcification. This resilience, however, is impaired when OA is combined with thermally induced reductions in the abundance of the coral's photosymbionts (i.e., 'bleaching'), which limits the extent to which the coral holobiont can utilize the elevated DIC via photosynthesis. These results highlight the threat that ocean warming and acidification pose for tropical and cold-water corals, especially when occurring in tandem.

**Supplementary Materials:** The following supporting information can be downloaded at: <https://www.mdpi.com/article/10.3390/jmse10081106/s1>: Summary of experimental design and results (Section S1); Water quality methods and summary tables (Section S2); Buoyant weight methods (Section S3); Images of calcein dye incorporation into coral skeleton (Section S4); Method for estimating photosymbiont index (Section S5); and Model summary tables (Section S6).

**Author Contributions:** Conceptualization, J.B.R. and R.A.E.; methodology, J.B.R., R.A.E., L.P.C., D.D.B., H.W., J.V.B., G.M.S.-G. and I.W.; formal analysis, L.P.C., J.B.R. and J.G.; investigation, L.P.C., J.B.R., C.E.R., F.M.-L., I.W., J.V.B. and R.A.E. sources, J.B.R., R.A.E., D.D.B., J.B. and H.W.; data curation, L.P.C., J.B.R. and R.A.E.; writing—original draft preparation, L.P.C. and J.B.R.; writing—review and editing, L.P.C., J.B.R., R.A.E., M.G., C.E.R., J.B., J.V.B., D.D.B., G.M.S.-G. and H.W.; visualization, L.P.C., J.B.R. and J.G.; supervision, J.B.R., R.A.E., D.D.B., J.B. and H.W.; project administration, J.B.R. and H.W.; funding acquisition, J.B.R., R.A.E. and H.W. All authors have read and agreed to the published version of the manuscript.

**Funding:** J.B.R. acknowledges support from National Science Foundation grant OCE-1437371, the ZMT, and a Hanse-Wissenschaftskolleg Fellowship. R.A.E. acknowledges support from National Science Foundation grant OCE-1437166, the Pritzker Endowment to UCLA IoES, and 'Laboratoire d'Excellence' LabexMER grant ANR-10-LABX-19 co-funded by a grant from the French government under the program 'Investissements d'Avenir'.

**Institutional Review Board Statement:** Not applicable.

**Informed Consent Statement:** Not applicable.

**Data Availability Statement:** It is our intention to make data available on publication of this study.

**Acknowledgments:** We thank Artur Fink, Laurie Hoffman, and Anja Niclas (MPIMM) for assistance with construction and use of pH microelectrodes; Silvia Hardenberg, Nico Steinel, and Christian Brandt (ZMT) for assistance with coral husbandry and redesign of the acidification system at the ZMT; and Matthias Birkicht (ZMT) for assistance with water chemistry analysis.

**Conflicts of Interest:** The authors declare no conflict of interest.

## References

1. IPCC. *Climate Change 2013—The Physical Science Basis*; Intergovernmental Panel on Climate Change, Ed.; Cambridge University Press: Cambridge, UK, 2014; ISBN 9781107415324. [[CrossRef](#)]
2. Caldeira, K.; Wickett, M.E. Anthropogenic carbon and ocean pH. *Nature* **2003**, *425*, 365. [[CrossRef](#)] [[PubMed](#)]



3. Ries, J.B.; Ghazaleh, M.N.; Connolly, B.; Westfield, I.; Castillo, K.D. Impacts of seawater saturation state state ( $\Omega_A = 0.4\text{--}4.6$ ) and temperature (10, 25 °C) on the dissolution kinetics of whole-shell biogenic carbonates. *Geochim. Cosmochim. Acta* **2016**, *192*, 318–337. [[CrossRef](#)]
4. Jokiel, P.L.; Rodgers, K.S.; Kuffner, I.B.; Andersson, A.J.; Cox, E.F.; Mackenzie, F.T. Ocean acidification and calcifying reef organisms: A mesocosm investigation. *Coral Reefs* **2008**, *27*, 473–483. [[CrossRef](#)]
5. Milliman, J.D. Production and accumulation of calcium carbonate in the ocean: Budget of a nonsteady state. *Glob. Biogeochem. Cycles* **1993**, *7*, 927–957. [[CrossRef](#)]
6. Anthony, K.R.; Fabricius, K.E. Shifting roles of heterotrophy and autotrophy in coral energetics under varying turbidity. *J. Exp. Mar. Biol. Ecol.* **2000**, *252*, 221–253. [[CrossRef](#)]
7. Hoegh-Guldberg, O. Climate change, coral bleaching and the future of the world's coral reefs. *Mar. Freshw. Res.* **1999**, *50*, 839–866. [[CrossRef](#)]
8. McCulloch, M.; Falter, J.; Trotter, J.; Montagna, P. Coral resilience to ocean acidification and global warming through pH up-regulation. *Nat. Clim. Change* **2012**, *2*, 623–627. [[CrossRef](#)]
9. Al-Horani, F.A.; Al-Moghrabi, S.M.; de Beer, D. The mechanism of calcification and its relation to photosynthesis and respiration in the scleractinian coral *Galaxea fascicularis*. *Mar. Biol.* **2003**, *142*, 419–426. [[CrossRef](#)]
10. Allison, N.; Finch, A.A. 11B, Sr, Mg and B in a modern *Porites* coral: The relationship between calcification site pH and skeletal chemistry. *Geochim. Cosmochim. Acta* **2010**, *74*, 1790–1800. [[CrossRef](#)]
11. Ries, J.B. A physicochemical framework for interpreting the biological calcification response to CO<sub>2</sub>-induced ocean acidification. *Geochim. Cosmochim. Acta* **2011**, *75*, 4053–4064. [[CrossRef](#)]
12. Venn, A.; Tambutté, E.; Holcomb, M.; Allemand, D.; Tambutté, S. Live tissue imaging shows reef corals elevate pH under their calcifying tissue relative to seawater. *PLoS ONE* **2011**, *6*, e20013. [[CrossRef](#)] [[PubMed](#)]
13. Comeau, S.; Cornwall, C.E.; McCulloch, M.T. Decoupling between the response of coral calcifying fluid pH and calcification to ocean acidification. *Sci. Rep.* **2017**, *7*, 7573. [[CrossRef](#)] [[PubMed](#)]
14. Sevilgen, D.S.; Venn, A.A.; Hu, M.Y.; Tambutté, E.; de Beer, D.; Planas-Bielsa, V.; Tambutté, S. Full in vivo characterization of carbonate chemistry at the site of calcification in corals. *Sci. Adv.* **2019**, *5*, eaau7447. [[CrossRef](#)] [[PubMed](#)]
15. Allison, N.; Cohen, I.; Finch, A.A.; Erez, J.; Tudhope, A.W. Corals concentrate dissolved inorganic carbon to facilitate calcification. *Nat. Commun.* **2014**, *5*, 5741. [[CrossRef](#)] [[PubMed](#)]
16. McCulloch, M.; D'Olivo, J.P.; Falter, J.; Holcomb, M.; Trotter, J.A. Coral calcification in a changing world and the interactive dynamics of pH and DIC upregulation. *Nat. Commun.* **2017**, *8*, 15686. [[CrossRef](#)]
17. Ries, J.B. Skeletal mineralogy in a high-CO<sub>2</sub> world. *J. Exp. Mar. Biol. Ecol.* **2011**, *403*, 54–64. [[CrossRef](#)]
18. Spalding, C.; Finnegan, S.; Fischer, W.W. Energetic costs of calcification under ocean acidification. *Glob. Biogeochem. Cycles* **2017**, *31*, 866–877. [[CrossRef](#)]
19. Castillo, K.D.; Ries, J.B.; Bruno, J.F.; Westfield, I.T. The reef-building coral *Siderastrea siderea* exhibits parabolic responses to ocean acidification and warming. *Proc. Biol. Sci.* **2014**, *281*, 20141856. [[CrossRef](#)]
20. Marubini, F.; Ferrier-Pages, C.; Furla, P.; Allemand, D. Coral calcification responds to seawater acidification: A working hypothesis towards a physiological mechanism. *Coral Reefs* **2008**, *27*, 491–499. [[CrossRef](#)]
21. Bove, C.B.; Ries, J.B.; Davies, S.W.; Westfield, I.T.; Umbanhowar, J.; Castillo, K.D. Common Caribbean corals exhibit highly variable responses to future acidification and warming. *Proc. Biol. Sci.* **2019**, *286*, 20182840. [[CrossRef](#)]
22. Ries, J.B.; Cohen, A.L.; McCorkle, D.C. A nonlinear calcification response to CO<sub>2</sub>-induced ocean acidification by the coral *Oculina arbuscula*. *Coral Reefs* **2010**, *29*, 661–674. [[CrossRef](#)]
23. Reynaud, S.; Leclercq, N.; Romaine-Lioud, S.; Ferrier-Pagès, C.; Jaubert, J.; Gattuso, J.-P. Interacting effects of CO<sub>2</sub> partial pressure and temperature on photosynthesis and calcification in a scleractinian coral. *Glob. Chang. Biol.* **2003**, *9*, 1660–1668. [[CrossRef](#)]
24. Comeau, S.; Cornwall, C.E.; DeCarlo, T.M.; Doo, S.S.; Carpenter, R.C.; McCulloch, M.T. Resistance to ocean acidification in coral reef taxa is not gained by acclimatization. *Nat. Clim. Chang.* **2019**, *9*, 477. [[CrossRef](#)]
25. Carafoli, E. Calcium signaling: A tale for all seasons. *Proc. Natl. Acad. Sci. USA* **2002**, *99*, 1115–1122. [[CrossRef](#)]
26. Mass, T.; Drake, J.L.; Peters, E.C.; Jiang, W.; Falkowski, P.G. Immunolocalization of skeletal matrix proteins in tissue and mineral of the coral *Stylophora pistillata*. *Proc. Natl. Acad. Sci. USA* **2014**, *111*, 12728–12733. [[CrossRef](#)]
27. Falini, G.; Fermani, S.; Goffredo, S. Coral biomineralization: A focus on intra-skeletal organic matrix and calcification. *Semin. Cell Dev. Biol.* **2015**, *35*, 17–26. [[CrossRef](#)]
28. Marin, F.; Smith, M.; Isa, Y.; Muyzer, G.; Westbroek, P. Skeletal matrices, muci, and the origin of invertebrate calcification. *Proc. Natl. Acad. Sci. USA* **1996**, *93*, 1554–1559. [[CrossRef](#)]
29. Westbroek, P.; Marin, F. A marriage of bone and nacre. *Nature* **1998**, *392*, 861–862. [[CrossRef](#)]
30. Mass, T.; Drake, J.L.; Haramaty, L.; Kim, J.D.; Zelzion, E.; Bhattacharya, D.; Falkowski, P.G. Cloning and characterization of four novel coral acid-rich proteins that precipitate carbonates in vitro. *Curr. Biol.* **2003**, *23*, 1126–1131. [[CrossRef](#)]
31. Mass, T.; Giuffrè, A.J.; Sun, C.-Y.; Stiffler, C.A.; Frazier, M.J.; Neder, M.; Tamura, N.; Stan, C.V.; Marcus, M.A.; Gilberg, P.U.P.A. Amorphous calcium carbonate particles form coral skeletons. *Proc. Natl. Acad. Sci. USA* **2017**, *114*, E7670–E7678. [[CrossRef](#)]
32. Hohn, S.; Reymond, C.E. Coral calcification, mucus, and the origin of skeletal organic molecules. *Coral Reefs* **2019**, *38*, 973–984. [[CrossRef](#)]



33. Roberts, J.M.; Wheeler, A.; Freiwald, A.; Cairns, S. *The Biology and Geology of Deep-Sea Coral Habitats*; Cambridge University Press: Cambridge, UK, 2009.
34. Hennige, S.J.; Wicks, L.C.; Kamenos, N.A.; Perna, G.; Findlay, H.S.; Roberts, J.M. Hidden impacts of ocean acidification to live and dead coral framework. *Proc. R. Soc. B* **2015**, *282*, 20150990. [[CrossRef](#)] [[PubMed](#)]
35. Büscher, J.V.; Form, A.U.; Riebesell, U. Interactive effects of ocean acidification and warming on growth, fitness and survival of the cold-water coral *Lophelia pertusa* under different food availabilities. *Front. Mar. Sci.* **2017**, *4*, 101. [[CrossRef](#)]
36. Georgian, S.E.; Dupont, S.; Kurman, M.; Butler, A.; Strömberg, S.M.; Larsson, A.I.; Cordes, E.E. Biogeographic variability in the physiological response of the cold-water coral *Lophelia pertusa* to ocean acidification. *Mar. Ecol.* **2016**, *37*, 1345–1359. [[CrossRef](#)]
37. Naumann, M.S.; Orejas, C.; Ferrier-Pagès, C. Species-specific physiological response by the cold-water corals *Lophelia pertusa* and *Madrepora oculata* to variations within their natural temperature range. *Deep. Sea Res. Part II Top. Stud. Oceanogr.* **2014**, *99*, 36–41. [[CrossRef](#)]
38. Holcomb, M.; Venn, A.A.; Tambutté, E.; Tambutté, S.; Allemand, D.; Trotter, J.; McCulloch, M. Coral calcifying fluid pH dictates response to ocean acidification. *Sci. Rep.* **2014**, *4*, 5207. [[CrossRef](#)]
39. Liu, Y.-W.; Sutton, J.N.; Ries, J.B.; Eagle, R.A. Regulation of calcification site pH is a polyphyletic but not always governing response to ocean acidification. *Sci. Adv.* **2020**, *6*, eaax1314. [[CrossRef](#)]
40. D’Olivo, J.P.; McCulloch, M.T. Response of coral calcification and calcifying fluid composition to thermally induced bleaching stress. *Nat. Sci. Rep.* **2017**, *7*, 2207. [[CrossRef](#)]
41. Guillermic, M.; Cameron, L.P.; De Corte, I.; Misra, S.; Bijma, J.; de Beer, D.; Reymond, C.E.; Westphal, H.; Ries, J.B.; Eagle, R.A. Thermal stress reduces pocilloporid coral resilience to ocean acidification by impairing control over calcifying fluid chemistry. *Sci. Adv.* **2021**, *7*, eaba9958. [[CrossRef](#)]
42. Ellison, J.C.; Fiu, M. Vulnerability of Fiji’s mangroves and associated coral reefs to climate change. *Ed. WWF S. Pac. Programme* **2010**, 50p.
43. Cameron, L.P.; Reymond, C.E.; Müller-Lundin, F.; Westfield, I.; Grabowski, J.H.; Westphal, H.; Ries, J.B. Effects of temperature and ocean acidification on the extrapallial fluid pH, calcification rate, and condition factor of the king scallop *Pecten maximus*. *J. Shellfish. Res.* **2019**, *38*, 763–777. [[CrossRef](#)]
44. Pierrot, D.; Lewis, E.; Wallace, D.W.R. MS excel program developed for CO<sub>2</sub> system calculations. In *ORNL/CDIAC-105a. Carbon Dioxide Information Analysis Center*; Oak Ridge National Laboratory U.S. Department Energy: Oak Ridge, TN, USA, 2006.
45. Siebeck, U.E.; Marshall, N.J.; Klüter, A.; Hoegh-Guldberg, O. Monitoring coral bleaching using a colour reference card. *Coral Reefs* **2006**, *25*, 453–460. [[CrossRef](#)]
46. Conti-Jerpe, I.E.; Thompson, P.D.; Wai Martin Wong, C.; Oliveira, N.L.; Duprey, N.N.; Moynihan, M.A.; Baker, D.M. Trophic strategy and bleaching resistance in reef-building corals. *Sci. Adv.* **2020**, *6*, eaaz5443. [[CrossRef](#)] [[PubMed](#)]
47. Morgans, C.A.; Hung, J.Y.; Bourne, D.G.; Quigley, K.M. Symbiodiniaceae probiotics for use in bleaching recovery. *Restor. Ecol.* **2020**, *28*, 282–288. [[CrossRef](#)]
48. De Beer, D.E.; Schramm, A.; Santegoeds, C.M.; Kühl, M. A nitrite microsensor for profiling environmental biofilms. *Appl. Environ. Microbiol.* **1997**, *63*, 973–977. [[CrossRef](#)]
49. Bates, D.; Mächler, M.; Bolker, B.; Walker, S. Fitting linear mixed-effects models using lme. *J. Stat. Softw.* **2015**, *67*, 1–48. [[CrossRef](#)]
50. Akaike, H. Factor analysis and AIC. In *Selected Papers of Hirotugu Akaike. Springer Series in Statistics (Perspectives in Statistics)*; Parzen, E., Tanabe, K., Kitagawa, G., Eds.; Springer: New York, NY, USA, 1987.
51. Houlbrèque, F.; Rodolfo-Metalpa, R.; Jeffree, R.; Oberhänsli, F.; Teyssié, J.-L.; Boisson, F.; Al-Trabeen, K.; Ferrier-Pagès, C. Effects of increased pCO<sub>2</sub> on zinc uptake and calcification in the tropical coral *Stylophora pistillata*. *Coral Reefs* **2012**, *31*, 101–109. [[CrossRef](#)]
52. Venn, A.A.; Tambutté, E.; Caminiti-Segonds, N.; Techer, N.; Allemand, D.; Tambutté, S. Effects of light and darkness on pH regulation in three coral species exposed to seawater acidification. *Sci. Rep.* **2019**, *9*, 2201. [[CrossRef](#)]
53. Rådecker, N.; Meyer, F.W.; Bednarz, V.N.; Cardini, U.; Wild, C. Ocean acidification rapidly reduces dinitrogen fixation associated with the hermatypic coral *Seriatopora hystrix*. *Mar. Ecol. Prog. Ser.* **2014**, *511*, 297–302. [[CrossRef](#)]
54. Cantin, N.E.; Cohen, A.L.; Karauskas, K.B.; Tarrant, A.M.; McCorkle, D.C. Ocean warming slows coral growth in the central Red Sea. *Science* **2010**, *329*, 322–325. [[CrossRef](#)]
55. Horvath, K.M.; Castillo, K.D.; Armstrong, P.; Westfield, I.T.; Courtney, T.; Ries, J.B. Next-century ocean acidification and warming both reduce calcification rate, but only acidification alters skeletal morphology of reef-building coral *Siderastrea siderea*. *Sci. Rep.* **2016**, *6*, 29639. [[CrossRef](#)] [[PubMed](#)]
56. Schoepf, V.; Grottole, A.G.; Warner, M.E.; Cai, W.-J.; Melman, T.F.; Hoadley, K.D.; Pettay, D.T.; Hu, X.; Li, Q.; Xu, H.; et al. Coral energy reserves and calcification in a high-CO<sub>2</sub> world at two temperatures. *PLoS ONE* **2013**, *8*, e75049. [[CrossRef](#)] [[PubMed](#)]
57. Okazaki, R.R.; Towle, E.K.; van Hooedonk, R.; Mor, C.; Winter, R.N.; Piggot, A.M.; Cunning, R.; Baker, A.C.; Klaus, J.S.; Swart, P.K.; et al. Species-specific responses to climate change and community composition determine future calcification rates of Florida Keys reefs. *Glob. Chang. Biol.* **2016**, *23*, 1023–1035. [[CrossRef](#)] [[PubMed](#)]
58. Hönisch, B.; Ridgwell, A.; Schmidt, D.N.; Gibbs, S.J.; Sluijs, A.; Zeebe, R.; Kump, L.; Martindale, R.C.; Greene, S.E.; Kiessling, W.; et al. The geologic record of ocean acidification. *Science* **2012**, *335*, 1058–1063. [[CrossRef](#)] [[PubMed](#)]
59. Bijma, J.; Pörtner, H.-O.; Yesson, C.; Rogers, A.D. Climate change and the oceans—What does the future hold? *Mar. Pollut. Bull.* **2013**, *74*, 495–505. [[CrossRef](#)]

60. Kurman, M.D.; Gómez, C.E.; Georgian, S.E.; Lunden, J.J.; Cordes, E.E. Intra-specific variation reveals potential adaptation to ocean acidification in a cold-water coral from the Gulf of Mexico. *Front. Mar. Sci.* **2017**, *4*, 111. [[CrossRef](#)]
61. Fabry, V.J.; McClintock, J.B.; Mathis, J.T.; Grebmeier, J.M. Ocean acidification at high latitudes: The bellwether. *Oceanography* **2009**, *22*, 160–171. [[CrossRef](#)]
62. Costello, M.J.; McCreagh, M.; Freiwald, A.; Lundälv, T.; Jonsson, L.; Bett, B.J.; van Weering, T.C.E.; de Haas, H.; Roberts, J.M.; Allen, D. Role of cold-water *Lophelia pertusa* coral reefs as fish habitat in the NE Atlantic. In *Cold-Water Corals and Ecosystems*. Erlangen Earth Conference Series; Freiwald, A., Roberts, J.M., Eds.; Springer: Berlin, Germany, 2005; pp. 771–805.
63. Mortensen, P.B.; Hovland, T.; Fossa, J.H.; Furevik, D.M. Distribution, abundance and size of *Lophelia pertusa* coral reefs in mid-Norway in relation to seabed characteristics. *J. Mar. Biol. Assoc. UK* **2001**, *81*, 581–597. [[CrossRef](#)]
64. Freiwald, A. Geobiology of *Lophelia pertusa* (scleractinia) reefs in the North Atlantic. Habilitation Thesis, University of Bremen, Bremen, Germany, 1998.
65. Rogers, A.D. The biology of *Lophelia pertusa* (Linnaeus 1758) and other deep-water reef-forming corals and impacts from human activities. *Int. Rev. Hydrobiol.* **1999**, *84*, 315–406. [[CrossRef](#)]
66. Dodds, L.A.; Roberts, J.M.; Taylor, A.C.; Marubini, F. Metabolic tolerance of the cold-water coral *Lophelia pertusa* (scleractinia) to temperature and dissolved oxygen change. *J. Exp. Mar. Biol. Ecol.* **2007**, *349*, 205–214. [[CrossRef](#)]
67. Fine, M.; Oren, U.; Loya, Y. Bleaching effect on regeneration and resource translocation in the coral *Oculina patagonica*. *Mar. Ecol. Prog. Ser.* **2002**, *234*, 119–125. [[CrossRef](#)]
68. Tambutté, E.; Allemand, D.; Zoccola, D.; Meibom, A.; Lotto, S.; Caminiti, N.; Tambutté, S. Observations of the tissue-skeleton interface in the scleractinian coral *Stylophora pistillata*. *Coral Reefs* **2007**, *26*, 517–529. [[CrossRef](#)]
69. Järnegren, J.; Kutti, T. *Lophelia pertusa* in Norwegian waters. What have we learned since 2008? *NINA Rep.* **2014**, *1028*, 40.
70. Davies, P.S. Short-term growth measurements of corals using an accurate buoyant weighing technique. *Mar. Biol.* **1989**, *101*, 389–395. [[CrossRef](#)]
71. Hennige, S.J.; Wolfram, U.; Wickes, L.; Murray, F.; Murray Roberts, J.; Kamenos, N.A.; Schofield, S.; Groetsch, A.; Spiesz, E.M.; Aubin-Tam, M.-E.; et al. Crumbling reefs and cold-water coral habitat loss in a future ocean: Evidence of “Coralporosis” as an indicator of habitat integrity. *Front. Mar. Sci.* **2020**, *7*, 668. [[CrossRef](#)]
72. Chan, N.C.S.; Connelly, S.R. Sensitivity of coral calcification to ocean acidification: A meta-analysis. *Glob. Chang. Biol.* **2013**, *19*, 282–290. [[CrossRef](#)]
73. Davies, S.W.; Marchetti, A.; Ries, J.B.; Castillo, K.D. Thermal and pCO<sub>2</sub> stress elicit divergent transcriptomic responses in a resilient coral. *Front. Mar. Sci.* **2016**, *3*, 112. [[CrossRef](#)]
74. Form, A.U.; Riebesell, U. Acclimation to ocean acidification during long-term CO<sub>2</sub> exposure in the cold-water coral *Lophelia pertusa*. *Glob. Chang. Biol.* **2012**, *18*, 843–853. [[CrossRef](#)]
75. Tanaka, K.; Holcomb, M.; Takahashi, A.; Kurihara, H.; Asami, R.; Shinjo, R.; Sowa, K.; Rankenburg, K.; Watanabe, T.; McCulloch, M. Response of *Acropora digitifera* to ocean acidification: Constraints from <sup>11</sup>B, Sr, Mg, and Ba compositions of aragonitic skeletons cultured under variable seawater pH. *Coral Reefs* **2015**, *34*, 1139–1149. [[CrossRef](#)]
76. Comeau, S.; Cornwall, C.E.; DeCarlo, T.M.; Krieger, E.; McCulloch, M.T. Similar controls on calcification under ocean acidification across unrelated coral reef taxa. *Glob. Chang. Biol.* **2018**, *24*, 4857–4868. [[CrossRef](#)]
77. Sutton, J.N.; Liu, Y.-W.; Ries, J.B.; Guillermic, M.; Ponzevera, E.; Eagle, R.A. <sup>11</sup>B as monitor of calcification site pH in divergent marine organisms. *Biogeosciences* **2018**, *15*, 1447–1467. [[CrossRef](#)]
78. Cai, W.-J.; Ma, Y.; Hopkinson, B.M.; Grottole, A.G.; Warner, M.E.; Ding, Q.; Hu, X.; Yuan, X.; Schoepf, V.; Xu, H.; et al. Microelectrode characterization of coral daytime interior pH and carbonate chemistry. *Nat. Commun.* **2016**, *7*, 11144. [[CrossRef](#)] [[PubMed](#)]
79. Cohen, A.L.; McConnaughey, T.A. Geochemical perspectives on coral mineralization. *Rev. Mineral. Geochem.* **2003**, *54*, 151–187. [[CrossRef](#)]
80. Kooijman, B. *Dynamic Energy Budget Theory for Metabolic Organization*; Cambridge University Press: Cambridge, UK, 2009.
81. Holcomb, M.; McCorkle, D.C.; Cohen, A.L. Long-term effects of nutrient and CO<sub>2</sub> enrichment on the temperate coral *Astrangia poculata* (Ellis and Solander, 1786). *J. Exp. Mar. Biol. Ecol.* **2010**, *386*, 27–33. [[CrossRef](#)]
82. Edmunds, P.J. Zooplanktivory ameliorates the effects of ocean acidification on the reef coral *Porites* spp. *Limnol. Oceanogr.* **2011**, *56*, 2402–2410. [[CrossRef](#)]
83. Gates, R.D.; Baghdasarian, G.; Muscatine, L. Temperature stress causes host cell detachment in symbiotic cnidarians: Implications for coral bleaching. *Biol. Bull.* **1992**, *182*, 324–332. [[CrossRef](#)]
84. Brading, P.; Warner, M.E.; Davey, P.; Smith, D.J.; Achterberg, E.P.; Suggett, D.J. Differential effects of ocean acidification on growth and photosynthesis among phylogenotypes of *Symbiodinium* (Dinophyceae). *Limnol. Oceanogr.* **2011**, *56*, 927–938. [[CrossRef](#)]
85. Moya, A.; Tambutté, S.; Bertucci, A.; Tambutté, E.; Lotto, S.; Vullo, D.; Supuran, C.T.; Allemand, D.; Zoccola, D. Carbonic anhydrase in the scleractinian coral *Stylophora pistillata* characterization, localization, and role in biomineralization. *J. Biol. Chem.* **2008**, *283*, 25475–25484. [[CrossRef](#)]
86. Chen, S.; Gagnon, A.C.; Adkins, J.F. Carbonic anhydrase, coral calcification and a new model of stable isotope vital effects. *Geochim. Cosmochim. Acta* **2018**, *236*, 179–197. [[CrossRef](#)]
87. Muscatine, L.; McCloskey, L.R.; Marian, R.E. Estimating the daily contribution of carbon from zooxanthellae to coral animal respiration. *Limnol. Oceanogr.* **1981**, *26*, 601–611. [[CrossRef](#)]

88. Dubinsky, Z.; Jokiel, P.L. Ratio of energy and nutrient fluxes regulates symbiosis between zooxanthellae and corals. *Pac. Sci.* **1994**, *48*, 313–324.
89. Aichelman, H.E.; Bove, C.B.; Castillo, K.D.; Boulton, J.M.; Knowlton, A.C.; Nieves, O.C.; Ries, J.B.; Davies, S.W. Exposure duration modulates the response of Caribbean corals to global change stressors. *Limnol. Oceanogr. Lett.* **2021**, *66*, 8. [[CrossRef](#)]
90. Cornwall, C.E.; Comeau, S.; DeCarlo, T.M.; Moore, B.; D'alexis, Q.; McCulloch, M.T. Resistance of corals and coralline algae to ocean acidification: Physiological control of calcification under natural pH variability. *Proc. R. Soc. B* **2018**, *285*, 20181168. [[CrossRef](#)]
91. Cohen, A.L.; Holcomb, M. Why corals care about ocean acidification: Uncovering the mechanism. *Oceanography* **2009**, *22*, 118–127. [[CrossRef](#)]
92. Allemand, D.; Ferrier-Pagès, C.; Furla, P.; Houlbrèque, F.; Puverel, S.; Reynaud, S.; Tambutté, É.; Tambutté, S.; Zoccola, D. Biomineralization in reef-building corals: From molecular mechanisms to environmental control. *Comptes Rendus Palevol* **2004**, *3*, 453–467. [[CrossRef](#)]
93. Gagliano, M.; McCormick, M.I.; Moore, J.A.; Depczynski, M. The basics of acidification: Baseline variability of pH on Australian coral reefs. *Mar. Biol.* **2010**, *157*, 1849–1856. [[CrossRef](#)]
94. Hofmann, G.E.; Smith, J.E.; Johnson, K.S.; Send, U.; Levin, L.A.; Micheli, F.; Paytan, A.; Price, N.N.; Peterson, B.; Takeshita, Y.; et al. High-frequency dynamics of ocean pH: A multi-ecosystem comparison. *PLoS ONE* **2011**, *6*, e28983. [[CrossRef](#)]
95. Cyronak, T.; Takeshita, Y.; Courtney, T.A.; DeCarlo, E.H.; Eyre, B.D.; Kline, D.I.; Martz, T.; Page, H.; Price, N.N.; Smith, J.; et al. Diel temperature and pH variability scale with depth across diverse coral reef habitats. *Limnol. Oceanogr. Lett.* **2019**, *5*, 193–203. [[CrossRef](#)]
96. Gray, S.E.C.; DeGrandpre, M.D.; Langdon, C.; Corredor, J.E. Short-term and seasonal pH, pCO<sub>2</sub> and saturation state variability in a coral-reef ecosystem. *Glob. Biogeochem. Cycles* **2012**, *26*, GB3012. [[CrossRef](#)]
97. Kline, D.I.; Teneva, L.; Hauri, C.; Schneider, K.; Miard, T.; Chai, A.; Marker, M.; Dunbar, R.; Caldeira, K.; Lazar, B.; et al. Six month in situ high-resolution carbonate chemistry and temperature study on a coral reef flat reveals asynchronous pH and temperature anomalies. *PLoS ONE* **2015**, *10*, e0127648. [[CrossRef](#)]